RESEARCH AND DEVELOPMENT OF A SYSTEMS MODEL OF A VIBRATORY BOWL FEEDER

A Thesis

Presented in Partial Fulfillment of the Requirements
for the Degree Master of Science

by

Robert Anthony Rejent, Jr., BSIE

The Ohio State University
1985

Approved by

Gary P. Maul

Adviser
Department of Industrial and
Systems Engineering

ACKNOWLEDGEMENTS

I would like to thank the people who were instrumental in helping me complete this thesis.

For guidance throughout my research, thanks go to Dr. Gary Maul and Dr. Richard Miller.

For completion of the final text, I thank Mrs. Annie Anderson.

Finally, I am especially grateful to my parents, without whose support and advice I would not have been able to complete this thesis or any of my education.

TABLE OF CONTENTS

LIST OF TABLES

LIST OF FIGURES

Chapter I

BACKGROUND

Manufacturing technology and practices in the 1980's are undergoing rapid change, both in industry and academia. Projections for the next decade predict that manufacturing will change more than it has in the past 50 years (19). Robotics and automation are sparking this change. Ten years ago, there were only a handful of robotic systems in operation. By 1981, there were over 22,000 robots in operation. In that year, the United States robotics industry was about a $94 million business; in 1985, the U.S. robotics industry is expected to become a $500 to $800 million business (13). Clearly, robotics and automation is the wave of the future in manufacturing.

The main reason for this trend to automation is productivity. Robots are more productive than human operators, due to their lack of fatigue, boredom, and environmental interactions which reduce human labor output. In addition, by utilizing more techniques of automation, the labor intensity of many products can be reduced, leading to higher productivity of labor per man hour (16).

One impediment, though, to the implementation of robotics strategies has been flexibility. Human laborers are much more flexible than robots. Screwing a bolt into a nut is an easy task for humans, but for a robot to perform the same task would require the use of vision, sensors, and extensive programming code. This lack of flexibility is a problem, since only 25% of manufacturing is mass-produced. The remaining 75% consists of batch manufacturing, meaning 50 to 100,000 pieces per year not manufactured on a continuous basis (16). Mass-produced work does not require flexibility in equipment, since the cost of dedicated tooling can be averaged over the high volume of parts made. Batch manufacturing, on the other hand, requires flexibility, since volumes for particular pieces are relatively low. This is where flexible manufacturing systems (FMS) come in.

Flexible manufacturing systems integrate robots into an automated system which can manufacture batch jobs profitably. Flexibility is achieved through designing tooling and equipment to handle part families, groups of parts related by geometry, rather than specific parts. One critical area in the reliable functioning of an FMS is parts feeding and orientation. In such an environment, minutes of downtime in a parts feeder translate into considerable dollars worth of lost production (2).

At assembly, robots must grasp a particular part to be inserted with a mating part. If this part is presented in random orientation to the robot, it must sense how the part is oriented to grasp it properly. This often requires spatial information obtained through the use of vision and sensors. This equipment is costly, and, due to it's recent development, performance is not nearly 100% reliable.

A simpler solution to presenting parts to robots is to orient them before the robot grasps them. The robot already expects the part in a certain orientation, so complex vision or sensing is not required for this operation. Parts feeders perform this function.

Parts feeders contain a relatively large bin of parts to be oriented. Through different orienting techniques, these parts are oriented properly and presented to the robot in a certain position. Parts feeders and devices can be grouped into several categories: magazines, disk feeders, reciprocating feeders, belt feeders, and vibratory feeders (23).

Magazines are containers that keep the orientation of parts directly after their manufacture. These devices replace conventional parts feeders and escapements, and down-time is nearly eliminated, since magazines are hooked directly to the placement mechanism of the robot. Magazines, however, cannot contain a large volume of parts, and must

constantly be refilled. Magazining is also limited by the manufacturing process of the robot.

Disk feeders are bin-of-parts feeders which are limited to feeding disk-shaped and cylindrical parts only. (See Figure 1.) Parts feeders of this type generally operate with some device which removes the part from the mass of parts, holding it in the correct orientation. For example, the rotary disk feeder contains a rotating wheel which directs oriented parts into slots in the wheel. Correctly oriented parts are then passed through the escapement chute to the robot. Disk feeders are often of this rotary type.

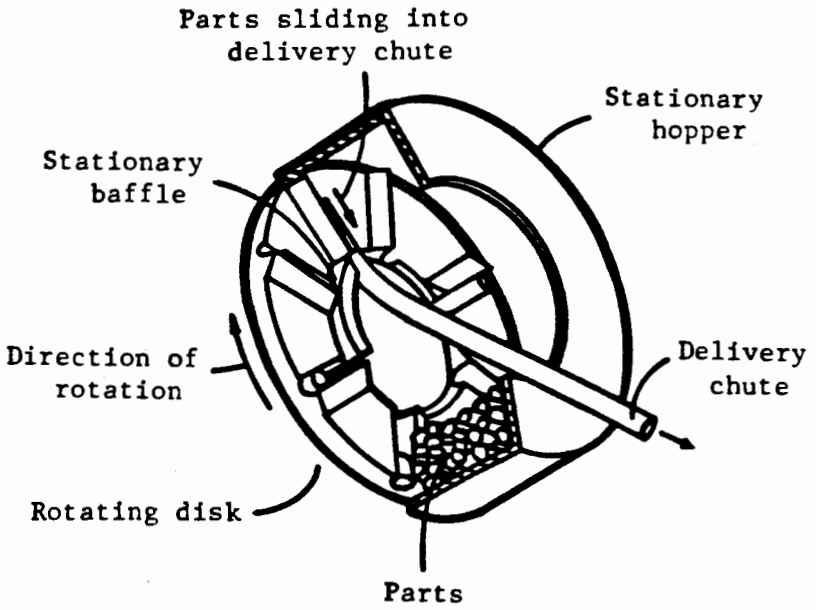

Figure 1: Rotary disk feeder

Reciprocating feeders operate on a different principle. In reciprocating feeders, a slotted blade is passed through a mass of parts in a bin, and only properly oriented parts

can align themselves in the blade and pass to the escapement chute. (See Figure 2.) This blade "reciprocates" back and forth, and parts are oriented each time. Again, these feeders are limited to parts of cylindrical shape.

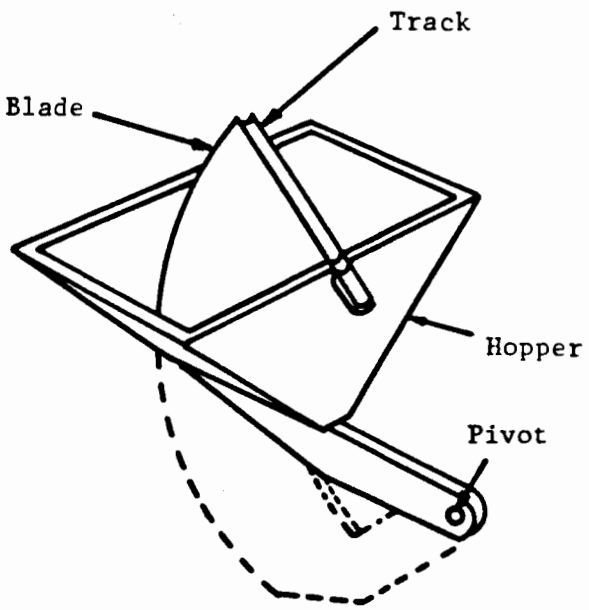

Figure 2: Centerboard hopper feeder

Belt feeders operate both vertically and horizontally. Vertically-operating belt feeders have slotted tracks or magnets on the belt in order to pick up parts. (See Figure 3.) The belt continuously passes through a bin of parts, and correctly oriented parts are picked up and moved up to the escapement chute, where they are discharged. Horizontally-operating belt feeders are usually bi-directional, and orient parts with successive tooling. Vertically-operating belt feeders are ideal for rings, cups, and similar-shaped parts (11), but horizontally-operating

feeders can feed many different types of parts. However, horizontally-operating feeders are just now being developed in industrial applications.

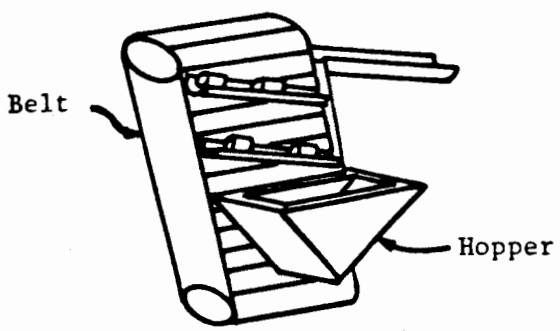

Figure 3: Elevator hopper feeder

Vibratory feeders use applied cyclical vibrations of the feed track to move parts through the feeder. By far, the most common is the vibratory bowl feeder (24). (See Figure 4.) Parts move around the track of the bowl and are oriented by devices along the track. These tools allow properly oriented parts to pass to the escapement chute, and reject other parts back to the bowl. Vibratory bowl feeders are the most versatile type of orienting device (6,20,21), and are also the most reliable of work handling mechanisms (1). They are widely used in industrial applications. In fact, these feeders are being used in flexible manufacturing systems. A

bowl feeder with simple vision has been developed (14), as well as a programmable bowl feeder for increased flexibility (12).

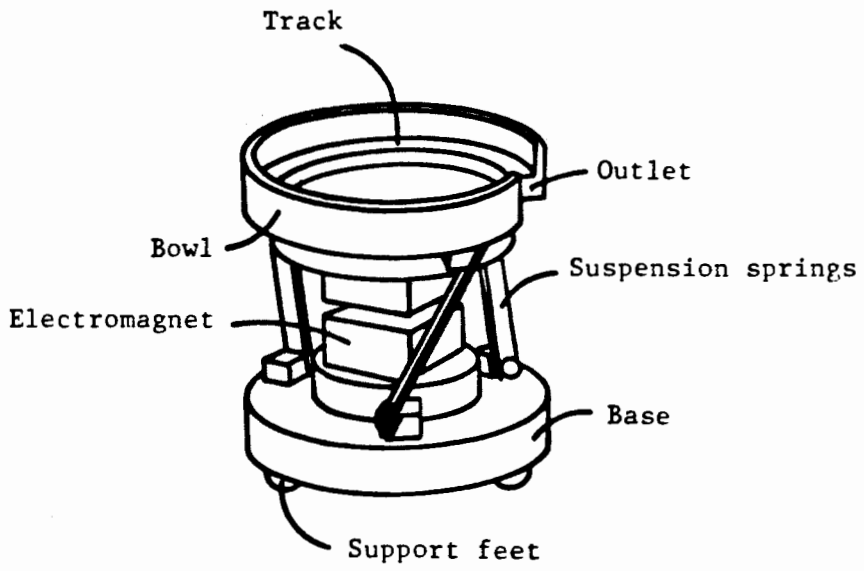

Figure 4: Vibratory bowl feeder

The bowl of the feeder is usually made of an aluminum alloy or stainless steel. Inside of the bowl along the inner wall is a helical track, leading from the bottom of the bowl to the top escapement chute, along which parts travel. Supporting the bowl are three leaf springs, inclined at an angle, which are mounted on the base. In the center of the base is an electromagnet. A voltage at a specified frequency is fed through a rectifier controller to the electromagnet. The coils in the electromagnet are cyclically energized and de-energized, which repeatedly attracts the bowl, then releases the bowl. Due to the constraining forces of the

spring, this creates a vibration around the bowl axis and a vertical vibration, creating a vertical and radial displacement of the part (4,17). In this manner, the parts move up the track.

Near the top of the track is where the orientation occurs. Active orientation requires the reorienting of all incorrectly positioned parts. Passive orientation requires the orienting device to allow only the correctly oriented parts to pass while all others are rejected back to the bowl, where they will be re-fed. In bowl feeders, the majority of orienting devices are passive, since parts can easily be rejected back to the bottom of the bowl. This orientation is performed by specific tooling and a variety of track configurations.

Tracks can have a variety of configurations to perform different functions. Pockets and dish-outs are holes cut into the track that reject parts which fall into them. (See Figure 5.) Dish-outs are cut into only half of the track, and allow only a single file of parts to pass. Pockets are cut into the track to the inside wall of the bowl, and tooling fits over these to reject incorrectly oriented parts through this pocket. Figure 6 show commonly-used track slopes, including positive track, negative track, hi-negative track, radius-form track, V-form track, slotted track, and flat track (22).

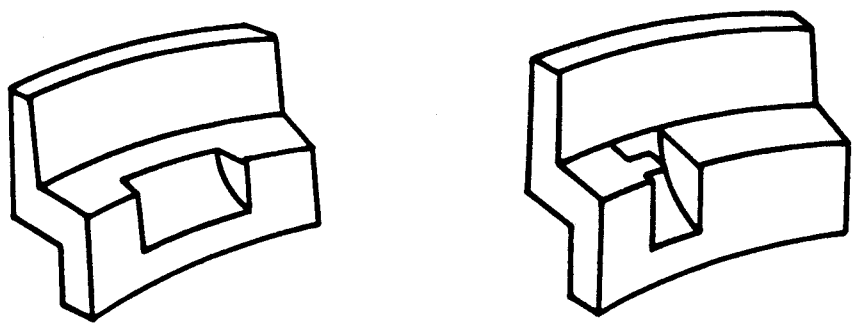

Figure 5: Dish-out and Pocket

A positive track is inclined toward the inside bowl wall, while a negative track is inclined toward the bottom of the bowl. Various angles can be specified. A hi-negative track uses a negative angle of 60 degrees to functionally return parts back to the bowl. The radius form track contains a semi-circular groove in the track, and the V-form track contains a V-groove in the track. Both are generally used for cylindrical parts. The slotted track contains a cut-out parallel to the bowl wall, and the flat track makes a 90-degree angle with the bowl wall.

Along with various track configurations, there are many types of tooling used in part orientation. The main types are shown in figure 7, and are described below.

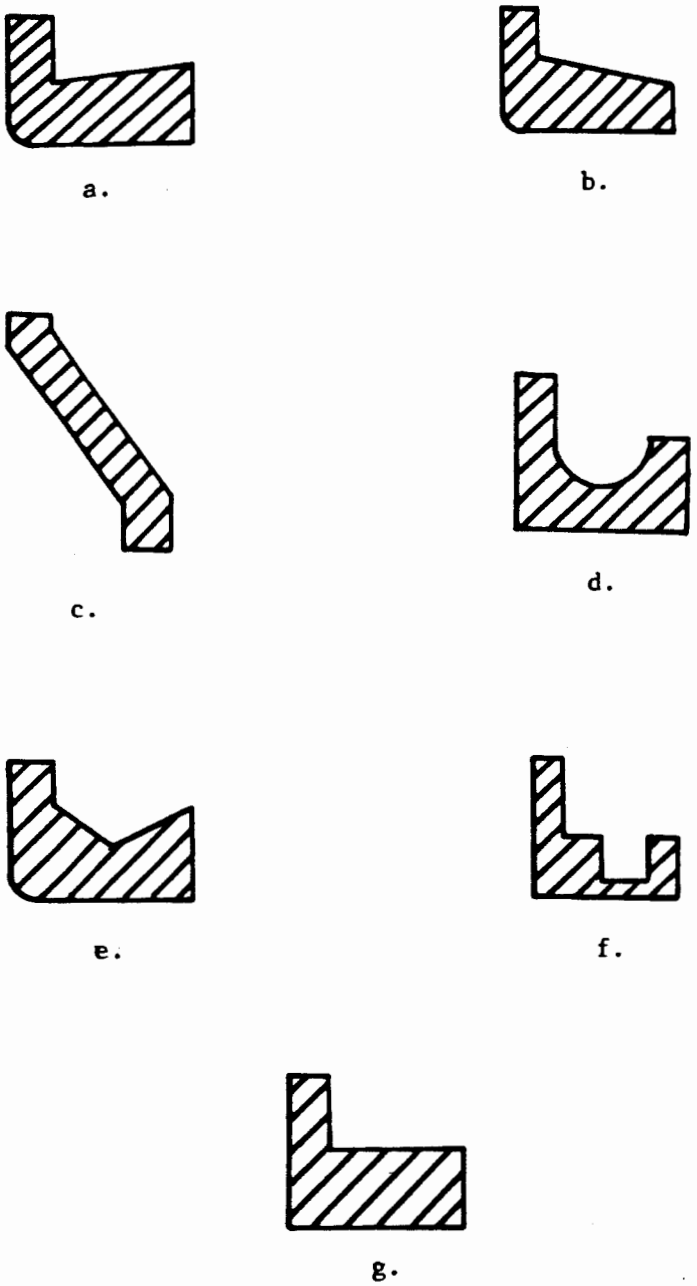

Figure 6: Track slope types. a) positive, b) negative, c) hi-negative, d) radius-form, e) v-form, f) slotted, and g) flat.

Wiper: A projection mounted at an angle to the bowl wall at an angle to the bowl wall at a height to allow only one thickness of parts to pass under it. This eliminates stacked parts.

Pressure Break: A narrow projection which relieves the pressure of parts lined up at the escapement chute by rejecting excess parts into the bowl. This helps to reduce track wear.

Retaining Rail: A shallow ledge placed at the edge of a negative track. Correctly oriented parts are upheld by the rail, while incorrectly oriented parts are rejected back to the bottom of the bowl.

Hold-Down: A tool positioned so as to maintain correct orientation of the part over a dish-out or negative track.

Roll-Up: A plane of increasing slope that guides parts from a horizontal to a vertical plane.

Scallops: A series of semicircular shapes placed over a pocket to allow cupped parts to pass only if they are resting on their bases. Otherwise, the open end catches and falls over one of the scallops and back into the bowl.

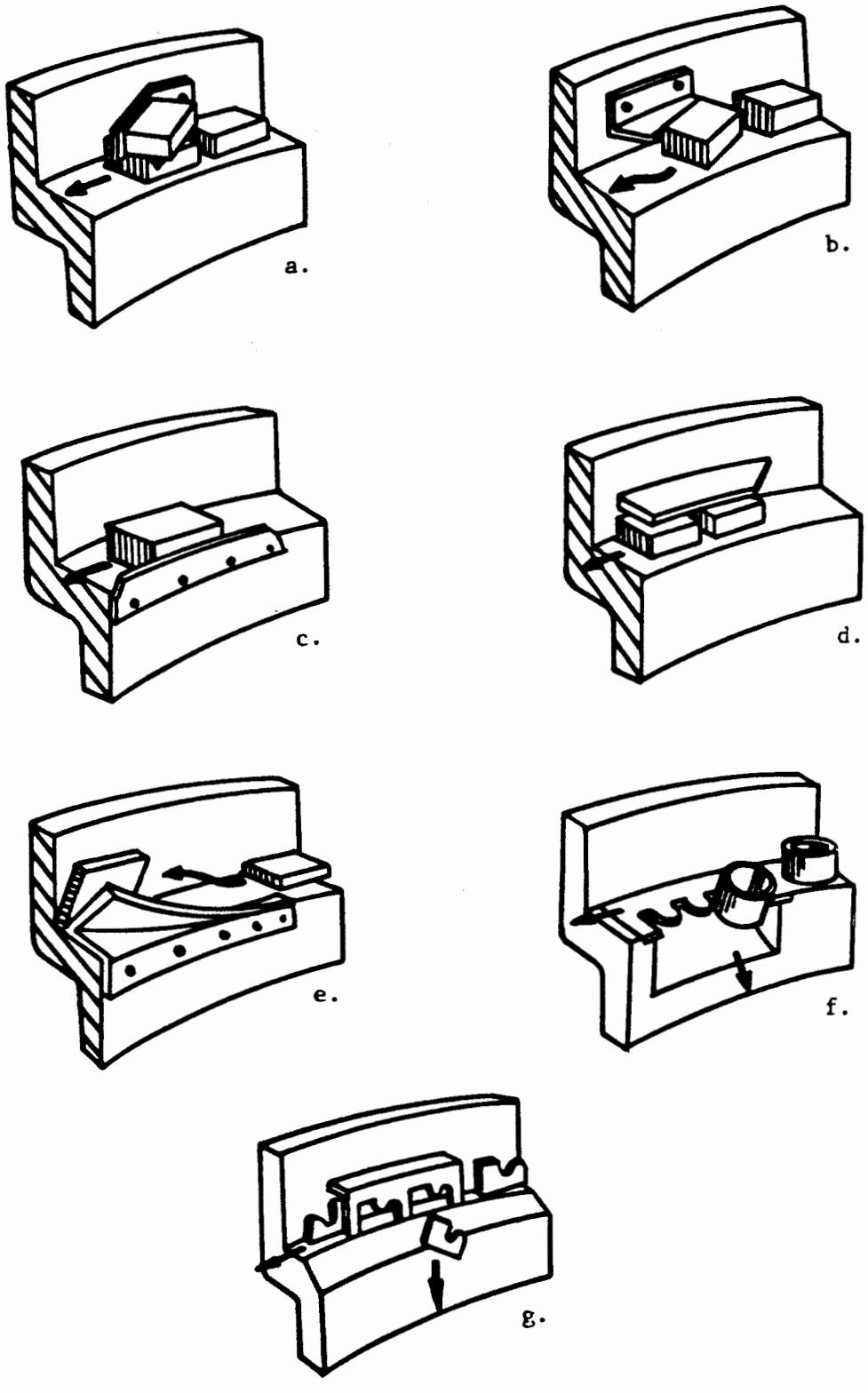

Figure 7: Tooling types. a) wiper, b) pressure break, retaining rail, d) hold-down, e)roll-up, scallop, and g) silhouette.

Silhouettes: Cut-outs in the shape of the part allow correctly oriented parts to pass, but parts which match the silhouette fall or are blown out and rejected into the bowl.

To show how these devices work together, an orienting system for flat rectangular parts in figure 8 is described. A positive track of 7 degrees is used here. The wiper allows only a single height of parts to pass, then the pressure break allows only a single file of parts to pass. The dish-out ensures a single file, and allows only parts passing lengthwise rather than sideways to pass. The hold-down and retaining rail keep parts oriented correctly until they reach the escapement chute.

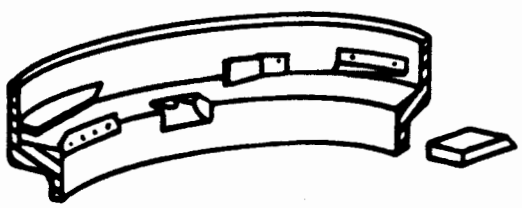

Figure 8: Orienting system for flat rectangular parts

Research has been done regarding the relationship of variables to the performance of a vibratory bowl feeder. Boothroyd and Redford have identified some of these variables as:

- o Frequency of vibration
- o Track acceleration
- o Vibration angle
- o Vibration amplitude
- o Track angle
- o Coefficient of friction between the part and the track
- o Load sensitivity in the bowl

They have developed individual relationships between these variables and part feed rates (7).

In industry, these relationships are not used on a regular and scientific basis to maintain bowl performance. In fact, in most applications of bowl feeders, experience and "black art" tend to govern the tuning of bowl parameters (3). More scientific principles must be applied to the operation of vibratory bowl feeders to improve the performance of these devices.

Very little work has been done modeling the total system of the bowl and looking at multiple-variable feeding relationships as a whole. The objective of this research is to fill in this scientific gap regarding the operation of bowl feeders.

Chapter II

MODEL DERIVATIONS

2.1 PARTS CONVEYANCE

The most important performance criteria for vibratory bowls is feed rate. The movement of a part along the bowl track is directly related to its feed rate, which is a measure of the output effectiveness of the bowl parameters. The position and movement of the part in relation to the track depends on such factors as friction and normal forces between the part and track. Once the part movement can be described using these variables, the total system of the bowl feeder can be modeled. This overall model will include relationships between the driving and mechanical components of the feeder, such as the electromagnet, springs, and bowl mass. In this section, the parts conveyance model will be developed and discussed. In section 2.2, the total systems model will be developed, using the parts conveyance model as one of its components.

The physical behavior of a part in a vibratory bowl feeder is not a concept that is agreed upon by the experts. Smith (21) and Treer (24) support the idea that the track is pulled downward and backward during each cycle. The part is

urged forward, then, by the track moving out from underneath the part. Boothroyd and Redford (7) support a different view. They claim that the part actually moves forward, either by sliding or hopping, and don't mention the actual movement of the track. Tipping (23) favors a movement described by both of these theories, but at different points in the conveyance cycle. These three theories of parts conveyance behavior will be described in detail.

The theory involving the active role of the track is the most straightforward of the theories. Figure 9 shows a basic cycle of part movement under this theory. In stage I, the cycle begins. The track is at the upper limit of its cyclical movement, and the part is resting on the track. The dot is used as a reference point for the initial position of the part. In stage II, the track is pulled downward and backward by the force of the electromagnet. Since the acceleration of the track in this direction is greater than the acceleration of the part (gravitational acceleration), the track is pulled away from the part. At this point, the part is directly above a portion of the track closer to the bowl outlet than the previous portion of the track it was resting on. In stage III, gravity pulls the part down to this advanced position of the track. In stage IV, the track completes the cycle, moving fully forward again. The part is

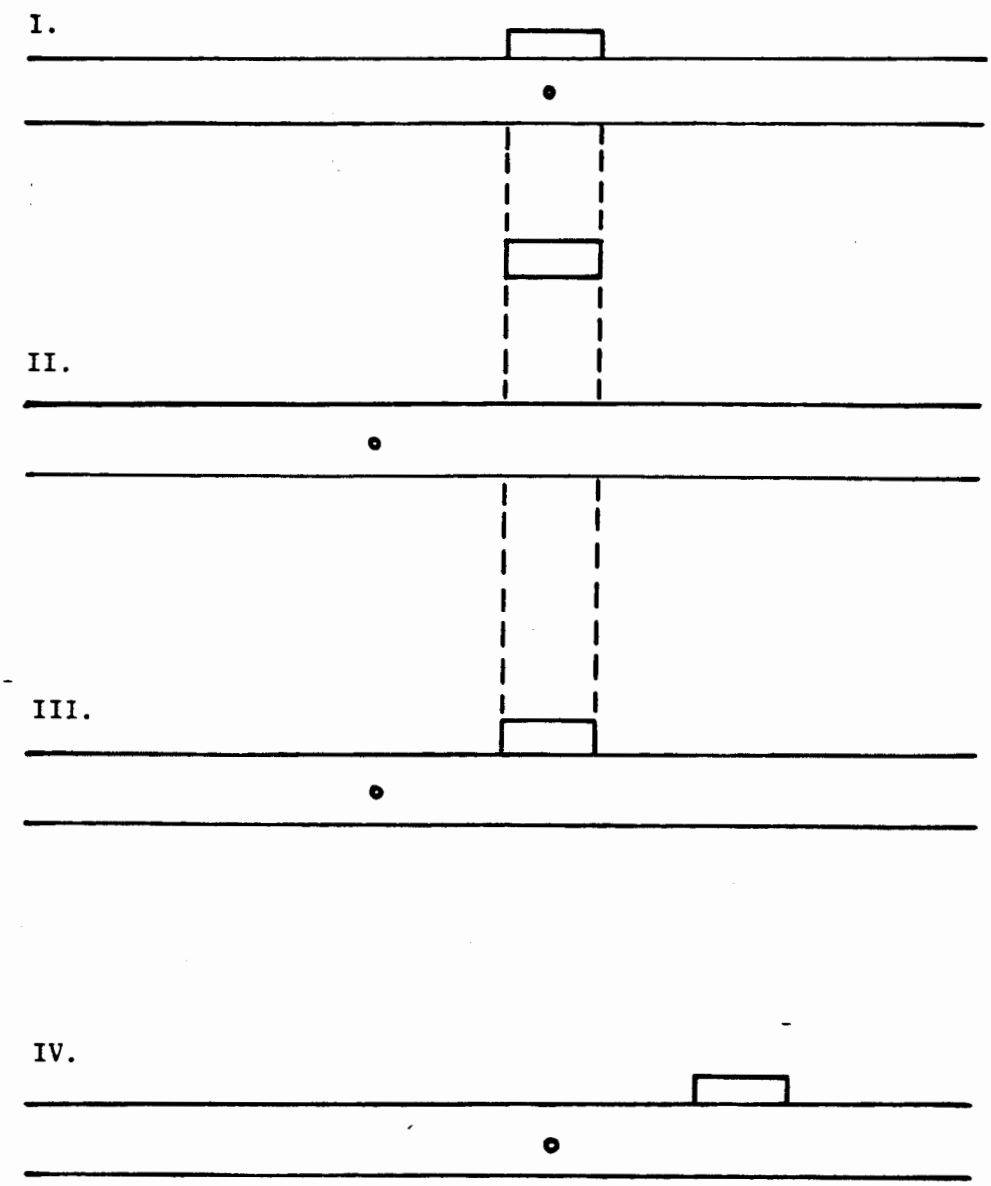

Figure 9: Active-track theory of parts conveyance behavior

now a fraction of an inch further along the track. The cycle repeats, causing the part to move along the track.

Boothroyd's theory on parts conveyance behavior places a much more active role on the part itself and the part/track interaction. He categorizes component motion into two distinct types. The first type involves continuous contact between the part and the track, which occurs when the acceleration perpendicular to the track cannot overcome the normal gravitational acceleration. Conveying of this type occurs due to sliding. The second type of component motion involves free flight. If the normal track acceleration is greater than the normal acceleration due to gravity, the part will "hop," and conveying will be due to a combination of hopping and sliding.

Figure 10 is a flow chart of the component conveying behavior as developed by Boothroyd and Redford (7). The part slides forward when the track is nearing the upper limit of its motion. If the normal track acceleration is greater than the normal gravitational acceleration, the component will then lose contact with the track, followed by a forward sliding motion when the contact is again made. If the normal track acceleration is less than the normal acceleration due to gravity, the part continues sliding forward until the track reaches the lower limit of its motion. At this point, the part may remain stationary until the cycle is complete,

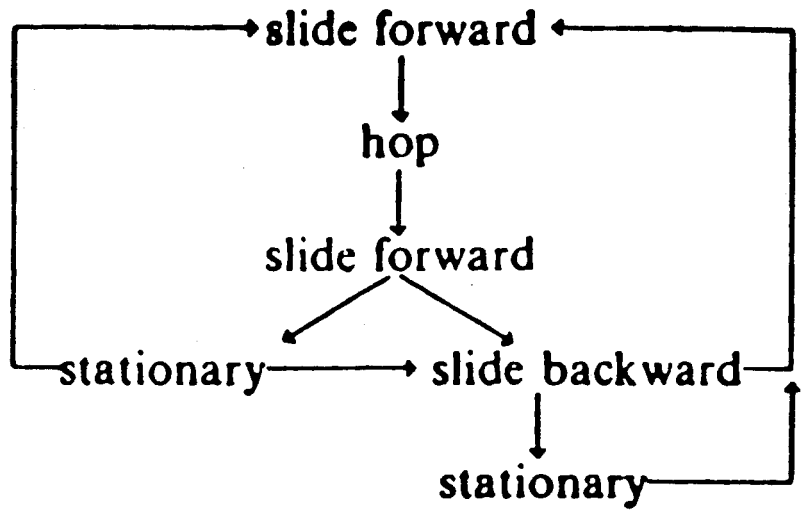

Figure 10: Boothroyd's theory of parts conveyance behavior (after Boothroyd and Redford (7))

or it may slide backward until the end of the cycle. In some cases, a stationary period is followed by backward sliding only or backward sliding followed by a stationary period. Finally, forward sliding may be followed by backward sliding and a stationary period. These combinations as shown in the flow chart are determined by part and track interactions, such as friction and track acceleration.

A third theory of parts conveyance behavior combines these two theories. Rather than treating the two previous theories as exclusive, this approach combines them. It can best be explained with reference again to figure 9. In stage

I, the part is in contact with the track. Under these conditions, the movement of the part is governed by the friction between the part and the track. Therefore, the part could slide forward, backward, or remain stationary, as described in Boothroyd's theory. In stage II the normal track acceleration is greater than gravitational acceleration perpendicular to the track, so the part can leave the track. In stage III, the track has slid under the component. This is the parts conveyance behavior described in the first theory involving the active role of the track, and also approximates Boothroyd's "hopping" motion. This motion would only occur when the normal track acceleration was greater than the normal acceleration due to gravity. Finally, in stage IV, the part has moved forward, due to part sliding (stage I), track movement under the part (stage II and III), or a combination of both. Although described in four possible stages of component conveyance, this theory is the most complicated, since sequences of movement depend on amplitude of vibration, frequency of vibration, friction, and relative accelerations of the part and track.

These theoretical explanations for parts conveyance behavior lead to the question: What is the conveyance behavior of parts at optimal operating conditions? From empirical experiments, DeCock has inferred that optimal feeder operation occurs when the normal track accleration is greater than the normal gravitational acceleration.

Therefore, he concluded that optimal feeding behavior occurs when parts hop off of the track and little or no sliding occurs.

A general approximation of parts behavior at standard conditions can be made using the distance equation:

$$s = \frac{1}{2}at^2 \qquad (1)$$

Where

s = Track amplitude of vibration

a = Track acceleration

t = Time

The acceleration of the track can be solved for using this equation and compared with gravitational acceleration. If the track acceleration is less than the gravitational acceleration of the part, then the part does not leave the track during conveyance. Using a standard amplitude of .025 inches (s=.025) and a standard frequency of 60 hertz (t=1/60 seconds), a value of a=15 feet per second squared is calculated. This is less than gravitational acceleration of 32.2 feet per second squared. Therefore, it appears that parts do not leave the track during conveyance under these standard conditions. Table 1 gives limiting values of amplitudes of vibration where track acceleration is less than acceleration due to gravity.

Table 1

Limiting conditions for no hopping to occur

frequency (hz)	amplitude of vibration (in)
30	.215
60	.054
120	.013

Since amplitudes are generally less than these values in practice, this analysis suggests that conveyance under standard conditions is accomplished mainly through part sliding.

These findings regarding parts conveyance behavior provide contradictory and inconclusive evidence as to how parts are conveyed under various conditions. A more specific model can be developed to determine actual distances parts move and accelerations of parts under a variety of different conditions. This can be done by investigating specific forces and interactions at the part/track interface to obtain a model for parts conveyance.

Figure 11 is a diagram of the part/track interface, with the forces acting on the block as shown. The symbols in the diagram represent:

F_f = Frictional force

m_p = Mass of part

g = Gravitational acceleration

F_p = Propelling force of part

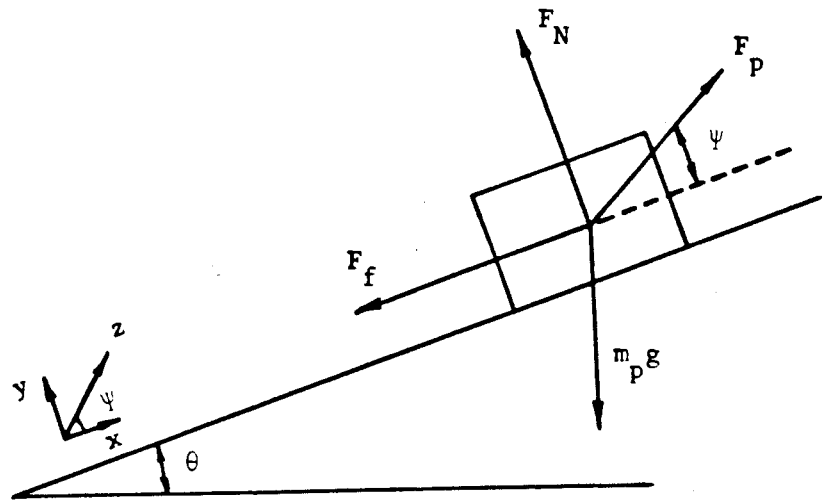

Figure 11: Part/track interface

F_N = Normal force

Ψ = Angle between the track and the line of vibration

θ = Inclination of the track

X = Distance parallel to track

Y = Distance normal to track

Z = Distance along angle Ψ

Note that the Z direction does not imply 3 dimensions, but is used only to describe the direction of motion along Ψ.

The frictional force, F_f, is defined as $\mu_S F_N$ for static relationships, where μ_S is the static coefficient of friction. When motion between the part and track exists, $F_f=\mu_K F_N$, where μ_K is the sliding coefficient of friction.

The weight of the part acts downwards, and is equal to $m_p g$. The propelling force, F_p, is imparted by the bowl to the part. The bowl can only impart a positive normal acceleration to the part, since the part is not attached to the bowl. This force is equal to the $m_p Z_1"(t)$, where $Z_1"(t)$ is the acceleration of the bowl along and t is a time index.

Finally, the normal force, F_N, can be determined by looking at the part/track interface in figure 12. The force imparted by the weight of the block normal to the track is $m_p g\cos\theta$, and the force imparted by the bowl is $m_p Z_1"(t)\sin\Psi$, looking at force directions in figure 11.

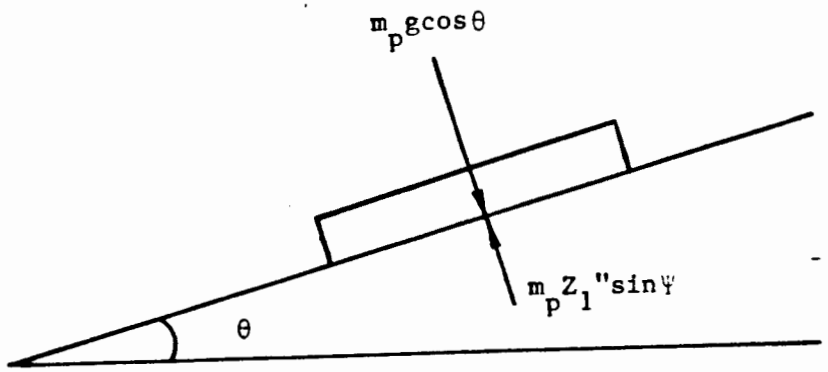

Figure 12: Determination of normal force

These forces are additive, since an increase in either force increases the contact force between the part and the track. Therefore, the normal force is:

$$F_N = m_p g\cos\theta + m_p Z_1''(t)\sin\psi \qquad (2)$$

F_N actually changes with time, and will be referred to as $F_N(t)$.

The acceleration of the part along the track plane is dependent on the frictional force. When the normal force is greater than zero, contact between the part and track exists, and the acceleration of the part can be described in one of three possible stages: forward part sliding, backward part sliding, or part stationarity.

For the part to move forward along the track, the velocity of the part must be greater than the velocity of the bowl along the track plane. In symbols:

$$Z_1'(t)\cos\psi < X_p'(t)$$

where

$Z_1'(t)$ = Velocity of bowl along ψ

$X_p'(t)$ = Velocity of part along the track

and $Z_1'(t)\cos\Psi$ is the velocity of the bowl along the track (derived by referring to figure 11). The equation for forward part motion can also be derived from figure 11. Equating forces parallel to the track, the force equation is:

$$m_p X_p''(t) = -m_p g \sin\Theta - \mu_K F_N(t) \tag{3}$$

One thing to note is that the drive force is not explicitly included in this equation, since it cannot impart a negative acceleration to the part. The acceleration of the bowl, however, is included in $F_N(t)$. The forward acceleration equation, from equation 3, is:

$$X_p''(t) = -g \sin\Theta - \frac{\mu_K F_N(t)}{m_p} \tag{4}$$

For the part to move backward along the track, the velocity of the part must be less than the velocity of the bowl along the track plane:

$$Z_1'(t)\cos\Psi > X_p'(t)$$

Referring to figure 11, for backward sliding, the frictional force is acting up the plane, and the force equation is:

$$m_p X_p''(t) = -m_p g \sin\Theta + \mu_K F_N(t) \tag{5}$$

which leads to:

$$X_p''(t)=-g\sin\theta+\frac{\mu_K F_N(t)}{m_p} \tag{6}$$

The part is stationary relative to the track when static friction is greater than the inertial force:

$$\mu_S F_N(t) > |F_I(t)|$$

Where $F_I(t)$ is the inertial force, equal to:

$$F_I(t)=m_p X_p''(t)+m_p g\sin\theta \tag{7}$$

The absolute value sign compensates for the direction of bowl movement. In this stationary case, the acceleration of the part and bowl along the track are equal, so:

$$X_p''(t)=Z_1''(t)\cos\Psi \tag{8}$$

If $F_N(t)$ is equal to zero, the part hops along the track. When the part leaves the track, the only force acting upon it is the force of gravity. The acceleration of a part in flight in a direction parallel to the track is:

$$X_p'' = -g\sin\theta \tag{9}$$

2.2 BOWL FEEDER SYSTEMS MODEL

To model the oscillitory motion of the bowl, the effect of the leaf springs on bowl vibrations had to be considered, since these springs allow for much of the bowl's motion. In addition, the springiness of the rubber base pads had to be looked at, since these also allow for some vibration. Therefore, a model with 2 degrees of freedom was chosen to represent the bowl feeder, as shown in figure 13.

In figure 13, the symbols are defined as:

m_1 = Mass of bowl

m_2 = Mass of base and electromagnet

k_1 = Spring constant of leaf springs

k_2 = Spring constant of rubber pads

b_1 = Damping coefficient of leaf springs

b_2 = Damping coefficient of rubber pads

Z_1 = Displacement of bowl

Z_2 = Displacement of base

The positive direction here is defined as downwards along the angle of vibration, ψ. To derive modeling equations for the bowl feeder, the forces acting on the bowl and the forces acting on the base were looked at separately. Systems dynamics concepts were applied to each component to develop these equations. Throughout the remaining derivations in

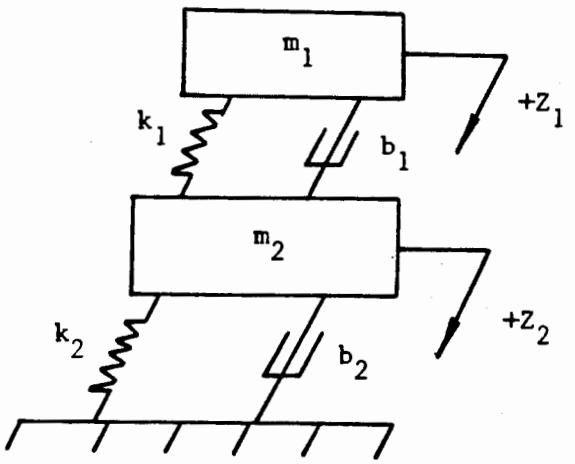

Figure 13: Systems model diagram

this Chapter, Z implies Z(t), but will not explicitly be written as a function of t for clarity in the derivations.

Figure 14 is a force diagram of the bowl. The actual forces on the bowl are:

$F_{K1} = k_1(Z_1-Z_2)$

$F_{b1} = b_1(Z_1'-Z_2')$

F_D = Drive force of the electromagnet

The velocity of the bowl and base are represented by Z_1' and Z_2', respectively, while the accelerations of each are represented by Z_1' and Z_2''.

The spring force, F_{K1}, was derived using the relation F=KX: the force of the spring is equal to the spring constant multiplied by the displacement of the spring. The

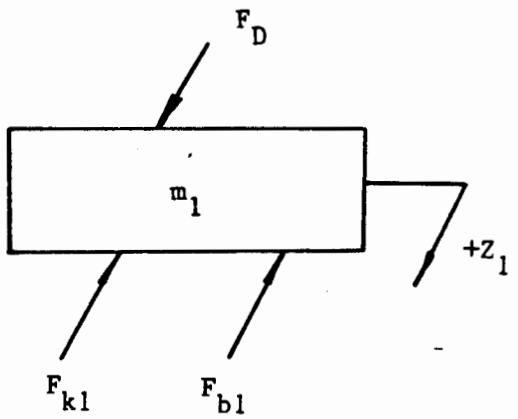

Figure 14: Bowl force diagram

damping force, F_{b1}, was derived using the relation F=bv: the damping force equals the damping coefficient times the velocity imparted to the damper. The actual form of the drive force, F_D, will be detailed in the next chapter, but can be assumed to be sinusoidal for the current derivation.

From Newton's law, the resultant force equation of the bowl motion is:

$$F_D - k_1(Z_1 - Z_2) - b_1(Z_1' - Z_2') = m_1 Z_1'' \qquad (10)$$

Dividing by m_1 gives the bowl acceleration as:

$$z_1'' = \frac{F_D}{m_1} - \frac{k_1}{m_1}(z_1-z_2) - \frac{b_1}{m_1}(z_1'-z_2') \qquad (11)$$

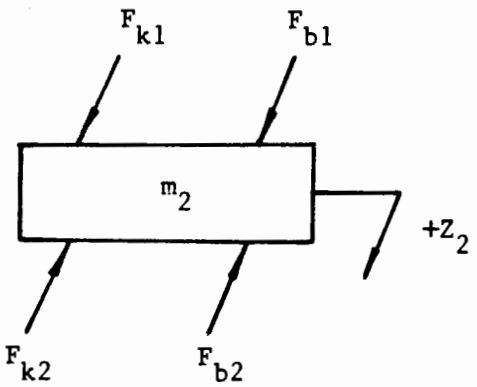

Figure 15: Base force diagram

Figure 15 is a force diagram of the base. These forces are:

$$F_{k2} = k_2 z_2$$
$$F_{b2} = b_2 z_2'$$

and F_{k1}, F_{b1} are as defined earlier. The resultant force equation of the base motion is:

$$k_1(z_1-z_2)+b_1(z_1'-z_2')-k_2z_2-b_2z_2'=m_2z_2'' \qquad (12)$$

Diving by m_2 gives the base acceleration as:

$$Z_2'' = \frac{k_1}{m_2}(Z_1-Z_2) + \frac{b_1}{m_2}(Z_1'-Z_2') - \frac{k_2}{m_2}Z_2 - \frac{b_2}{m_2}Z_2' \qquad (13)$$

These two differential equations describe the motion of the bowl system. The acceleration of the bowl, Z_1'', is the propelling acceleration to the part, as explained earlier in this chapter when deriving the part propelling force. The bowl acceleration, then, is how the motion of the bowl is linked to the motion of the part along the bowl track.

The objective of this research is to determine the velocity of a part in a bowl given certain parameters. Therefore, these equations derived for bowl and part motion must be solved. Chapter 3 describes the solution methods used, as well as a computer simulation of the solution techniques.

Chapter III

SOLUTION METHODOLOGY

The equations derived in Chapter 2 for part motion and bowl oscillation must now be integrated to determine the actual part feed rate. To accomplish this integration, the bowl velocity, $Z_1'(t)$, and acceleration, $Z_1''(t)$, must be solved for in order to determine the displacement of the part, $X_p(t)$, as well as its velocity, $X_p'(t)$. The method chosen to solve for these variables was Euler's approximation.

Euler's approximation is a mathematical technique used in solving differential equations. The solution method uses an approximation of the derivative to estimate values of a dependent variable at successive time points. Take the following differential equation:

$$\underline{U}'(t)=A\underline{U}(t)+B\underline{V}(t) \qquad (14)$$

where

$\underline{U}(t)$ = Vector of dependent variables

$\underline{U}'(t)$ = Vector of derivatives of $\underline{U}(t)$

$\underline{V}(t)$ = Vector of additive variables

A,B = Matrix of independent variable coefficients

The approximation of the derivative states that:

$$\underline{U}'(t) \approx \frac{\underline{U}(t+\Delta)-\underline{U}(t)}{\Delta} \tag{15}$$

where delta (Δ) is a very small time increment. The derivative of a variable is equal to the rate of change of that variable when delta is very small. Substituting this into equation 14 gives:

$$\frac{\underline{U}(t+\Delta)-\underline{U}(t)}{\Delta} \approx A\underline{U}(t)+B\underline{V}(t) \tag{16}$$

Solving for $\underline{U}(t+\Delta)$, the final result is:

$$\underline{U}(t+\Delta) \approx (I+A\Delta)\underline{U}(t)+\Delta B\underline{V}(t) \tag{17}$$

where I is the identity matrix. This procedure can be used iteratively in a simulation program to obtain values of $\underline{U}(t+\Delta)$, the dependent variable vector, at future points in time given $\underline{U}(0)$.

Solutions of the bowl equations were first calculated. The acceleration equations for the bowl and base were derived in Chapter 2 (equations 11 and 13). The dependent variable vector, $\underline{U}(t)$, is defined as:

$$U_1(t) = Z_1(t) \tag{18}$$

$$U_2(t) = Z_1'(t) \tag{19}$$

$$U_3(t) = Z_2(t) \tag{20}$$

$$U_4(t) = Z_2'(t) \tag{21}$$

Substituting this $\underline{U}(t)$ vector into equations 11 and 13, the derivative vector, $\underline{U}'(t)$, is:

$$U_1'(t)=Z_1'(t)=U_2(t) \tag{22}$$

$$U_2'=Z_1''(t)=-\frac{k_1}{m_1}U_1(t) - \frac{b_1}{m_1}U_2(t) + \frac{k_1}{m_1}U_3(t)+\frac{b_1}{m_1}U_4(t) + \frac{F_D}{m_1} \tag{23}$$

$$U_3'(t)=Z_2'(t)=U_4(t) \tag{24}$$

$$U_4'(t) = Z_2''(t) = \frac{k_1}{m_2}U_1(t) + \frac{b_1}{m_2}U_2(t) + \frac{(-k_1-k_2)}{m_2}U_3(t) + \frac{(-b_1-b_2)}{m_2}U_4(t) \tag{25}$$

In matrix form,

$$\begin{bmatrix} U_1'(t) \\ U_2'(t) \\ U_3'(t) \\ U_4'(t) \end{bmatrix} = \begin{bmatrix} 0 & 1 & 0 & 0 \\ -k_1/m_1 & -b_1/m_1 & k_1/m_1 & b_1/m_1 \\ 0 & 0 & 0 & 1 \\ k_1/m_2 & b_1/m_2 & (-k_1-k_2)/m_2 & (-b_1-b_2)/m_2 \end{bmatrix}$$

$$x \begin{bmatrix} U_1(t) \\ U_2(t) \\ U_3(t) \\ U_4(t) \end{bmatrix} + \begin{bmatrix} 0 \\ F_D/m_1 \\ 0 \\ 0 \end{bmatrix}$$

This is in the form of Euler's approximation in equation 14. By analogy, then, this matrix can be used to derive $\underline{U}(t)$ values at later points in time. Using equation 17, this becomes:

$$\underline{U}(t+\Delta) \approx \begin{bmatrix} 1 & \Delta & 0 & 0 \\ \frac{-k_1\Delta}{m_1} & \frac{(m_1-b_1\Delta)}{m_1} & \frac{k_1\Delta}{m_1} & \frac{b_1\Delta}{m_1} \\ 0 & 0 & 1 & \Delta \\ \frac{k_1\Delta}{m_2} & \frac{b_1\Delta}{m_2} & \frac{(-k_1-k_2)\Delta}{m_2} & \frac{(m_2+(-b_1-b_2)\Delta}{m_2} \end{bmatrix} *$$

$$\underline{U}(t) + \begin{bmatrix} 0 \\ \frac{\Delta F_D}{m_1} \\ 0 \\ 0 \end{bmatrix}$$

Finally, in equation form, this can be written:

$$U_1(t+\Delta) \approx U_1(t) + \Delta U_2(t) \qquad (26)$$

$$U_2(t+\Delta) \approx \frac{-k_1\Delta}{m_1}U_1(t) + \frac{(m_1-b_1\Delta)}{m_1}U_2(t) + \frac{k_1\Delta}{m_1}U_3(t)$$

$$+ \frac{b_1\Delta}{m_1}U_4(t) + \frac{F_D\Delta}{m_1} \qquad (27)$$

$$U_3(t+\Delta) \approx U_3(t) + \Delta U_4(t) \qquad (28)$$

$$U_4(t+\Delta) \approx \frac{k_1\Delta}{m_2}U_1(t) + \frac{b_1\Delta}{m_2}U_2(t)$$

$$+ \frac{(-k_1k_2)\Delta}{m_2}U_3(t) + \frac{(m_2+(-b_1-b_2)\Delta)U_4(t)}{m_2} \qquad (29)$$

These equations were then used in a simulation program to approximate the vibratory motion of the bowl feeder.

To determine the velocity and displacement of the part, the acceleration equations derived in Chapter 2 for the part/track interface were next solved. The velocity of the bowl, $Z_1'(t)$, which was just solved for, can now be integrated into this solution.

The variables to be solved for in the part/track interface are:

$X_p(t)$ = Cumulative displacement of part

$X_p'(t)$ = Velocity of part

The solution method used to solve for these variables was again Euler's approximation, and was used to determine these variables for both forward and backward sliding, as well as for part hopping. For clarity, a $\underline{W}$ vector will replace the $\underline{U}$ vector in the derivation. The dependent variable vector is:

$$W_1(t) = X_p(t) \tag{30}$$

$$W_2(t) = X_p'(t) \tag{31}$$

For forward sliding, the equation for part acceleration was derived in equation 4. Using that equation, the derivative vector for forward sliding is:

$$W_1'(t) = X_p'(t) = W_2(t) \tag{32}$$

$$W_2'(t) = X_p''(t) = -g\sin\theta - \frac{\mu_k F_N(t)}{m_p} \tag{33}$$

By following the same derivation used to develop the $\underline{U}$ matrix in equations 22 through 29, the final equations for forward motion are:

$$W_1(t+\Delta) \simeq W_1(t) + \Delta W_2(t) \tag{34}$$

$$W_2(t+\Delta) \simeq W_2(t) - \Delta g\sin\theta - \frac{\Delta\mu_k F_N(t)}{m_p} \tag{35}$$

and, from equation 4,

$$X_p''(t+\Delta) = -g\sin\theta - \frac{\mu_K F_N(t+\Delta)}{m_p} \tag{36}$$

For backward sliding, equation 6 is used in determining the derivative vector:

$$W_1'(t)=X_p'(t)=W_2(t) \tag{37}$$

$$W_2'(t) = X_p''(t) = -g\sin\theta + \frac{\mu_k F_N(t)}{m_p} \tag{38}$$

Using the same method as above, the final equations are:

$$W_1(t+\Delta)\approx W_1(t)+\Delta W_2(t) \tag{39}$$

$$W_2(t+\Delta)\approx W_2(t)-\Delta g\sin\theta + \frac{\Delta\mu_k F_N(t)}{m_p} \tag{40}$$

$$X_p''(t+\Delta) = -g\sin\theta + \frac{\mu_k F_N(t+\Delta)}{m_p} \tag{41}$$

For the stationary case, Euler's approximation is not necessary, since the motion of the bowl completely governs the motion of the part. The equations of motion in the stationary case are:

$$X_p(t+\Delta) = Z_1(t+\Delta)\cos\Psi \tag{42}$$

$$X_p'(t+\Delta) = Z_1'(t+\Delta)\cos\Psi \tag{43}$$

$$X_p''(t+\Delta) = Z_1''(t+\Delta)\cos\Psi \tag{44}$$

To make X_p cumulative in the stationary case, Euler's approximation was used to determine displacement. This equation is:

$$X_p(t+\Delta) \approx X_p(t)+\Delta X_p'(t) \tag{45}$$

which is analagous to equations 34 and 39 for part displacement in the forward and backward cases. This approximation is accurate since $X_p'(t)$ is defined using the bowl velocity as in equation 43.

During the hopping stage, X_p is interpreted as the distance the part moves through the air in the X direction. For this stage,

$$W_1'(t) = X_p'(t) = W_2(t) \tag{46}$$

$$W_2'(t) = X_p''(t) = -g\sin\theta \tag{47}$$

Applying Euler's approximation to this results in:

$$W_1(t+\Delta) \approx W_1(t) + \Delta W_2(t) \tag{48}$$

$$W_2(t+\Delta) \approx W_2(t) - \Delta g \sin\theta \tag{49}$$

which describes the part position and velocity along the direction of the track.

The solution methods for bowl and part motions were implemented using a computer simulation. Independent parameters were input through user interaction. The Fortran program listing and documentation can be found in the Appendix. The basic flow of the program begins with parameter inputs and conversions. All angles are converted to radians for computational purposes. The mass of the bowl, m_1, is converted to include the mass of the bowl and parts:

$$m_1 = m_1 + (m_p \times (\#\ \text{parts})) \tag{50}$$

m_1 is not a dynamic variable in the program, since the mass is not lessened by parts leaving the bowl. However, this does not really effect the simulation, since run times used to approximate feed rates are not long enough to significantly decrease total part weight in the bowl.

After conversions, the program goes into a loop indexed by time. Values for bowl motion are first calculated using the $\underline{U}(t+\Delta)$ equations derived earlier. These values are then used in determining part motion. Values of $Z_1'(t)$ and $Z_1''(t)$

are corrected for sign differences in going from the bowl reference frame to the part/track frame, since positive directions are switched.

The stages for part motion along the track are determined in the program from part and bowl velocities as

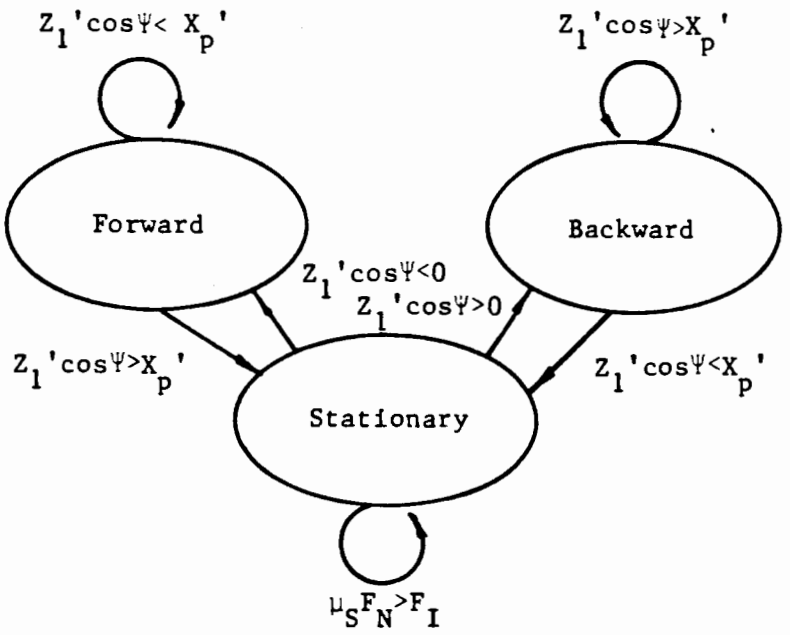

Figure 16: Stage transitions for part (No hopping)

shown in figure 16. Given a part is moving forward, it will move forward in the next time period (Δ seconds) if the velocity of the part is greater than that of the bowl along the direction of the track. Otherwise, the part will be stationary on the next cycle. This occurs because for a part

to change from forward to backward motion, it must be stationary between transitions.

If a part is moving backwards, it will continue to move backwards if the velocity of the bowl is greater than that of the part. Otherwise, the next cycle will be stationary.

A part will remain stationary if the static friction is greater than the inertial force. When the part breaks from the stationary mode, it is assumed that its motion is opposite in direction to the motion of the bowl. In the simulation program, if the velocity of the bowl is positive, the part motion is determined to be backwards in the next stage. Otherwise, the motion is forward.

The part hops along the track if the normal force becomes nonpositive. If this condition is detected during any stage of part motion, the part will leave the track. The motion of the part will continue in this stage until the position of the part normal to the track is equal to the position of the bowl. Therefore, the position, Y_p, and velocity, Y_p', of the part in the y direction had to be accumulated. While on the track, the part's position and velocity are equal to that of the bowl:

$$Y_p(t) = Z_1(t)\sin\Psi \tag{51}$$

$$Y_p'(t) = Z_1'(t)\sin\Psi \tag{52}$$

When the part leaves the track, the acceleration of the part normal to the track is:

$$Y_p'' = -g\cos\theta \tag{53}$$

Using Euler's approximation, the normal position and velocity of the part are:

$$Y_p(t+\Delta) \approx Y_p(t) + \Delta Y_p'(t) \tag{54}$$

$$Y_p'(t+\Delta) \approx Y_p'(t) - \Delta g\cos\theta \tag{55}$$

When the y position of the part and track are equal, the forward sliding stage is next entered. The collision of the part and track is assumed to be inelastic, so any part bouncing after impact is unaccounted for.

The remainder of the program keeps track of part and bowl velocities and accelerations. An additional subroutine computes the drive force, F_D. The actual form of the wave is half-rectified, as in figure 17a. Only the positive portion of the wave is passed on to the electromagnet. This wave form is approximated in the simulation as a step function, as in figure 17b.

The subroutine outputs a new voltage force after every 1/2f time increment, where f is the frequency. The value is either zero or the voltage force, calculated from actual data in chapter 4.

When running the simulation, a delta of .0001 seconds was used in order to accurately approximate the derivative at high frequencies. A limit of 1 second was used since feed rates were observed to stabilize well before this point.

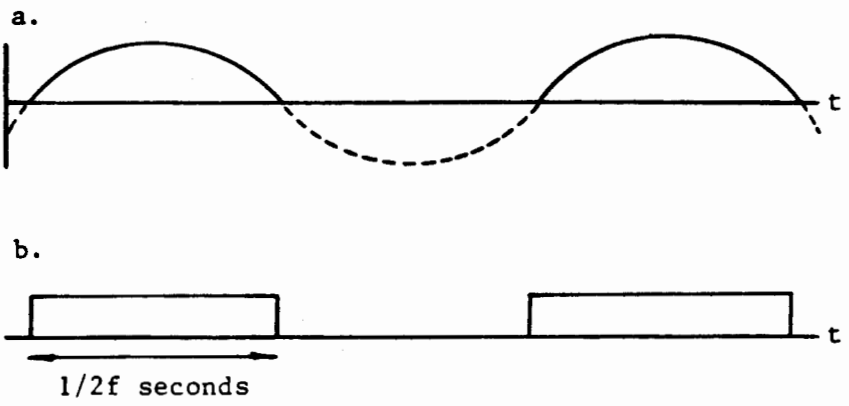

Figure 17: a) Sinusoidal half-rectified wave
b) Step approximation

In order to use the program to describe a physical feeder, the bowl parameters, k_1, k_2, b_1, b_2, had to be determined. The experimental determination of these data is detailed in chapter 4.

Chapter IV

EXPERIMENTAL DETERMINATION OF BOWL PARAMETERS

To use the simulation program, data had to first be gathered on the bowl parameters. Some parameters were easily determined. The weight of the bowl is 20 pounds, and the base weighs 58 pounds. The vibration angle, Ψ, was measured by resting a protractor on the base of the feeder where the spring is mounted. By substracting this measurement from 90 degrees (since the vibration is perpendicular to the springs), Ψ was found to be 17 degrees. The track angle was measured as 3 degrees at the bowl surface and lower track intersection. The frequency of the input is nominally set at 60 hertz.

Other parameters were more difficult to determine. The static coefficient of friction, μ_s, and kinetic coefficient of friction, μ_k, were difficult to find exactly. An experimental method described by Freier (10) used to determine μ_s involved the relation:

$$\mu_s = \tan \alpha \tag{56}$$

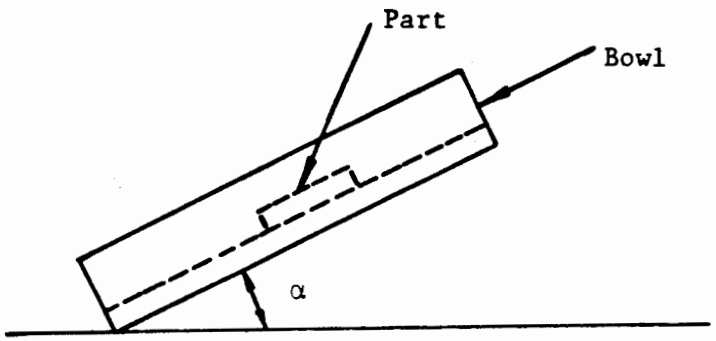

Figure 18: Determination of μ_s

where α is the angle at which a stationary part on an incline begins to slide. Figure 18 shows α as the angle between the titled bowl surface and the horizontal reference plane. Using this setup, μ_s was calculated as .91.

This still leaves μ_k unknown. Using Marks' Handbook (5), a value of μ_s and μ_k for mild steel on lead is:

$$\mu_s = .95$$
$$\mu_k = .90$$

Due to the relative closeness of the experimental value and handbook value for μ_s, the handbook values for μ_s and μ_k were used in the simulation.

The leaf spring constant, k_1, was measured with a spring scale as shown in figure 19. The leaf springs were

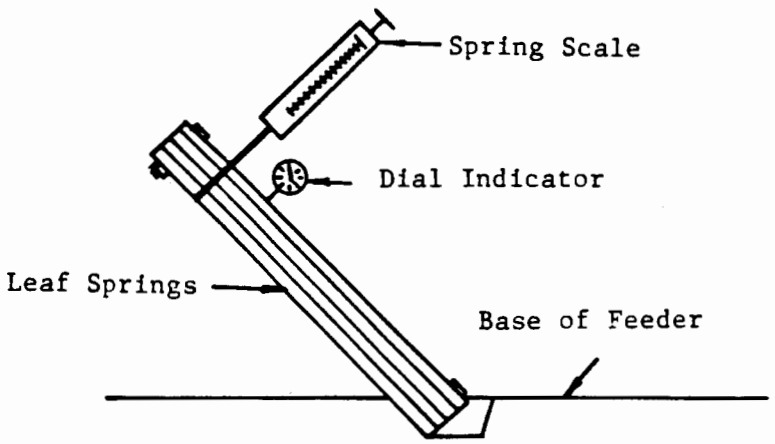

Figure 19: Measurement of K_1

bolted together without being attached to the bowl. The spring scale was put directly below the bolt nut and pulled perpendicular to the spring with gradually increasing force. This was measured on the scale in pounds. A dial indicator was placed on the surface of the spring to measure the displacement. The spring constant, then, was calculated by dividing the pulling force by the displacement:

$$k_1 = \frac{\text{force}}{\text{displacement}} \equiv \frac{\text{pounds}}{\text{inch}} \qquad (57)$$

Fourteen readings were taken at displacement intervals of .0025 inches. The spring constant for one leaf spring was found to be 1764 pounds per inch. Since three springs in parallel are used to support the bowl, the effective spring constant, k_1, is;

$$k_1 = 3x1764\frac{lbs}{in} = 5292\ \frac{lbs}{in} \tag{58}$$

In measuring k_2, the spring constant of the rubber base pads, the dial indicator was again used to measure displacement as shown in figure 20. The indicator was zeroed above the base, and weights were placed in the center of the base. k_2 was measured to be 10569 pounds per inch.

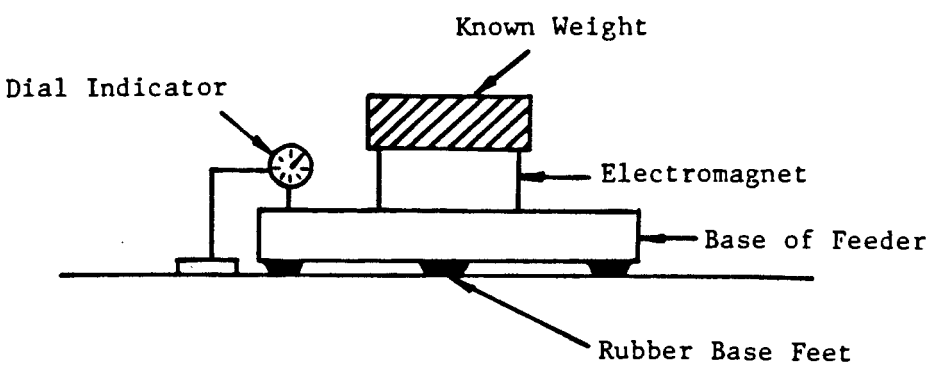

Figure 20: Measurement of k_2

The damping coefficients of the bowl, b_1, and the base, b_2, were measured using an accelerometer. The accelerometer was mounted to the bowl or base and hooked up to a strip

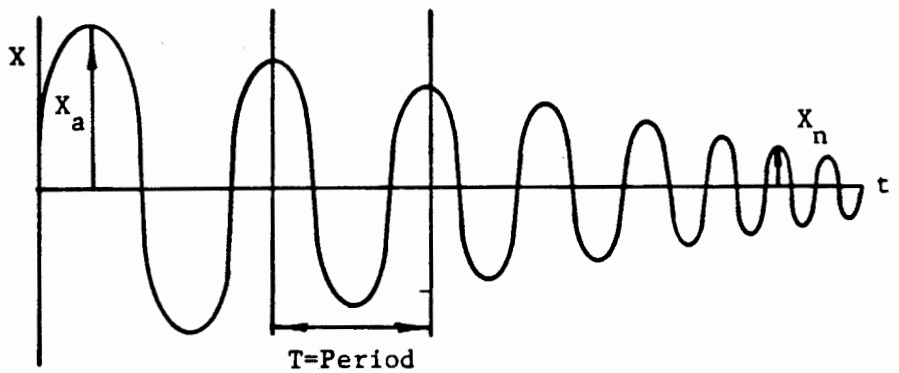

Figure 21: Damping behavior

chart recorder. To measure the damping coefficients, an experimental procedure described by Reswick and Taft (18) was followed. Using this method, successive periods of oscillation were counted and amplitude values recorded at each endpoint, as in figure 21. To determine the damping coefficients, 2 equations were used:

$$\zeta = \frac{\ln(X_a/X_n)}{2\Pi n} \tag{59}$$

$$b = 2\zeta\sqrt{km} \tag{60}$$

where

X_a = Amplitude value of first oscillation

X_n = Amplitude value of n^{th} oscillation

n = Number of periods

ζ = Damping ratio

k = Spring constant

m = Mass of system

b = Damping coefficient

To determine b_1, the damping of the springs, 4 readings were taken after striking the bowl with a hammer. In order to accurately measure the damping in the springs without other vibrational interference, the rubber base feet were removed. Parameters plugged into equation 60 were k_1 and m_1, and b_1 was averaged as .33 lb.-sec./inch over four readings. To measure b_2, the accelerometer was placed on the base and vibrations recorded. The bowl was removed in this phase in order to accurately measure the damping in the rubber feet only. Using parameters k_2 and m_2, b_2 was calculated as .258 lb.-sec./inch.

The final parameter to be measured was the force of the electromagnet, F_D. This is the force which the magnet pulls

on the steel plate beneath the bowl base. To measure this force, a dynamometer was set up as in figure 22.

The dynamometer was mounted to a platform above the bowl magnet. It was linked to a charge amplifier and strip chart recorder to measure output force. Mounted to the dynamometer was a 1-inch thick aluminum block. This block prevented any outside magnetic forces from influencing the true attractive force between the magnet and the steel plate. Mounted below the aluminum block was the steel plate of the bowl base. It was placed at a gap setting of .020 inches above the bowl magnet. To prevent any deflection of the plate, which would effect true force readings, 2 aluminum posts were placed between the aluminum block and the bowl base. With this setup, the magnet was energized for various dial settings, and the forces measured. Table 2

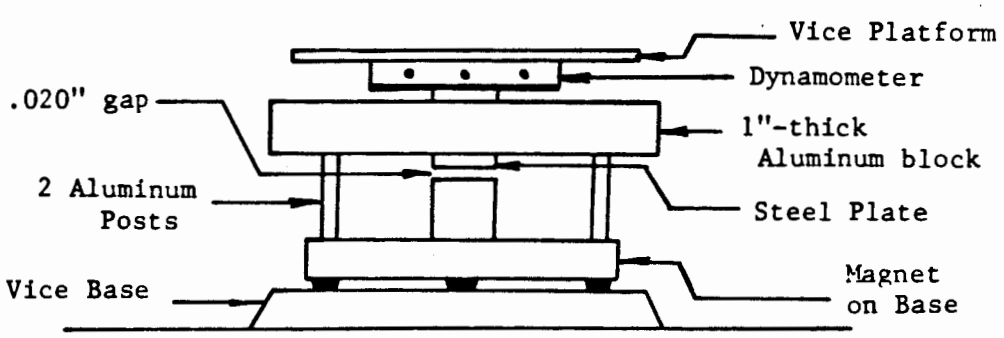

Figure 22: Measurement of F_D

shows the amplitude force values at different voltage settings.

TABLE 2
Force Measurements

Voltage Dial Settings	Force (lbs)
2	3.48
4	11.58
6	31.47
8	49.46
10	83.75

To facilitate ease of input, the voltage settings are input into the program and converted to magnetic forces. The data above was used to obtain a regression equation so that any setting input could be converted to a voltage force. this data is parabolic in form, so the fitted regression line was a second degree polynomial. Using the matrix equation (from Box and Hunter (8)):

$$\hat{b} = [X'X]^{-1}X'Y \tag{61}$$

where

$\hat{b}$ = Estimate of coefficients in regression line

X = Voltage settings matrix

Y = Force vector

the following regression curve was calculated:

$$Y = 1.724 - .896X + .901X^2 \tag{62}$$

this conversion is implemented in the program.

As mentioned in chapter 4, a step function was used to approximate the drive force. In reality, the force is implemented as a duty cycle, where only parts of the wave are output. Figure 23 shows how the effective portion of the wave is to the right of the firing point. For large

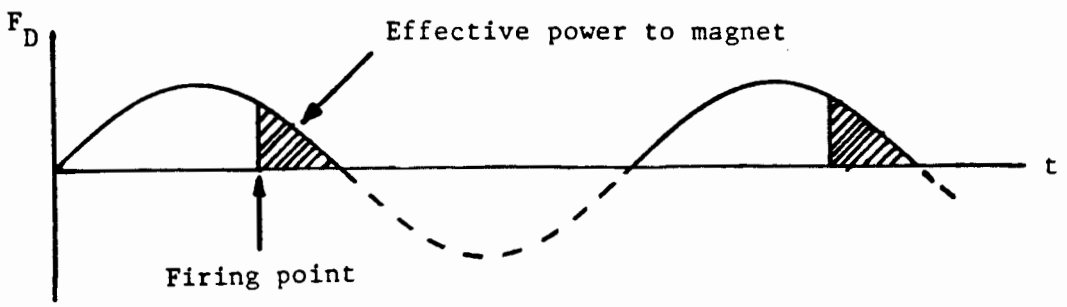

Figure 23: Actual waveform of F_D

settings, this point moves left until most of the sinusoidal wave is applied to the electromagnet. The actual power is represented by the shaded area.

The step function was used as an approximation since effective power in figure 23 is the same for a specified voltage setting. Although temporal patterns change, the firing point is the same for each setting, so the step function is a reasonable drive input approximation. A half-rectified wave was not used since measurements of the

forces (see Table 2) correspond with average voltage forces over the duty cycle. Since the exact firing point for each dial setting was difficult to determine, a sinusoidal waveform could not be used. Therefore, the step function was found to most closely approximate these average force measurements.

Now that bowl parameters have been determined, the simulation model must be tested on the actual bowl to determine how accurate the model can predict part velocities.

Chapter V

MODEL VERIFICATION

To test the accuracy of the simulation model, six different weights of parts were fed in the bowl feeder and their velocities measured at various controller settings. These parts and their weights are listed in Table 3.

TABLE 3
Weights of Tested Parts

Part Type	Weight (pounds)
Cotter Pins	.00125
Crimp Terminals	.00625
1/4" Hex Nuts	.01250
5/16" Screw	.02500
5/8" Screw	.18125
3/4" Screw	.30000

The feeding velocity of each part was measured on the bowl feeder for controller settings ranging from 0 to 10 in increments of .5. For each part type, 25 parts were placed in the bowl during these verification tests. For each measurement, one part was placed on the top bowl track and its speed measured over a distance of 18 inches. This 18 inches was measured directly before the bowl outlet. Velocity measurements were averaged over 3 readings and plotted in the graphs presented in figures 24 through 31.

The simulation program was then run using the bowl feeder parameters reported in chapter 4. These parameters are summarized in table 4. Using this data resulted in bowl

TABLE 4
Bowl parameters

Symbol	Name	Value
μ_s	Coefficient of static friction	.95
μ_k	Coefficient of kinetic friction	.90
m_1	Mass of bowl	20 lbs.
m_2	Mass of base	58 lbs.
k_1	Spring constant, springs	5292 lbs/inch
k_2	Spring constant, rubber feet	10569 lbs/inch
b_1	Damping coefficient, springs	.33 lb-sec/inch
b_2	Damping coefficient, rubber feet	.258 lb-sec/ inch
f	Frequency	60 hz
Ψ	Vibration angle	17 degrees
Θ	Track angle	3 degrees
Δ	Time interval	.0001 sec.
limit	Total simulation time	1 sec.

displacements approximately one inch in amplitude, which is far greater than actual bowl vibrations. An analysis of the data suggested that b_1 and b_2 may not be accurate measurements of the damping in the springs and rubber feet, respectively. When measuring b_1 and b_2, outside vibrational damping effects may have been included in the readings of the damping effects of the springs and rubber base pads. This would tend to reduce the measured effects of damping in the spring and feet. Therefore, values of b_1 greater than .33 pound-seconds per inch and greater than .258

pound-seconds per inch were input into the program. To properly tune the damping coefficient values with the bowl performance, the data from a medium-weight part, the hex nut, was matched with output from the simulation program. By comparing values for this size of part at a controller setting of 7, the closest correlation of actual bowl data to simulation data occurred for a b_1 value of 8.2 lb.-sec./inch and a b_2 value of 6.4 lb.-sec./inch. These values were used for all of the simulation runs. The ratio of b_1 to b_2 values is the same for both simulated and experimental data in order to use as much information from the experimental measurements as possible.

The velocity graphs for each of the six different part types are presented in figures 24 through 29. Each graph shows the actual and simulated velocities for a range of controller settings from 0 to 10. Overall, the simulation model is much more sensitive to changes in mass than the actual bowl. Velocities in the actual bowl feeder decrease by about 1/4 when comparing the lightest part, the cotter pins, to the heaviest part, the 3/4" diameter screw. Velocities calculated by the simulation model decrease by a factor of about 20 over this same range. The simulation is also more sensitive to changes in the controller setting than the actual bowl. The simulation curves for the four lightest parts are steeper than the measured curves, which shows this sensitivity to voltage input.

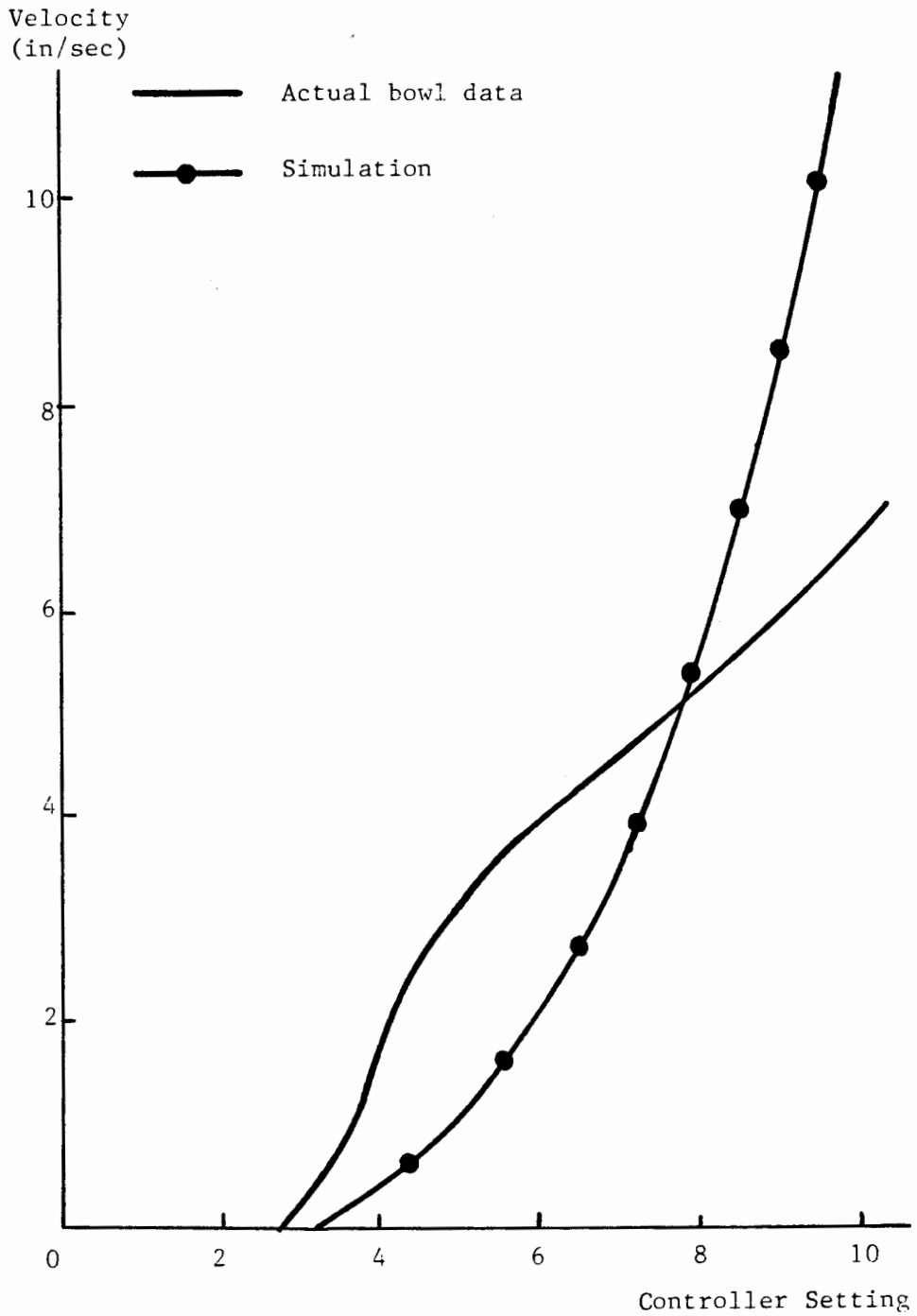

Figure 24: Velocity graph for cotter pins

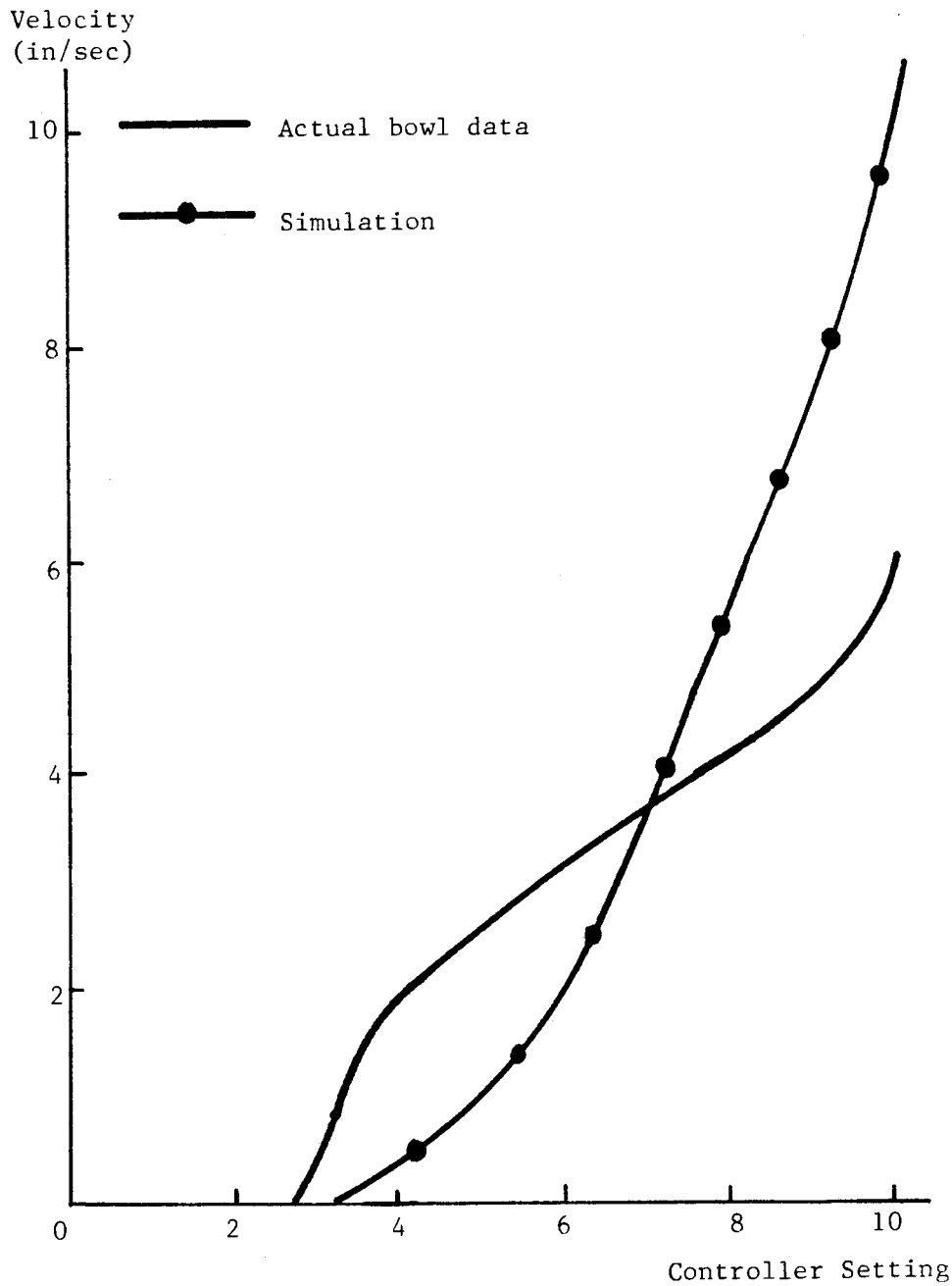

Figure 25: Velocity graph for crimp terminals

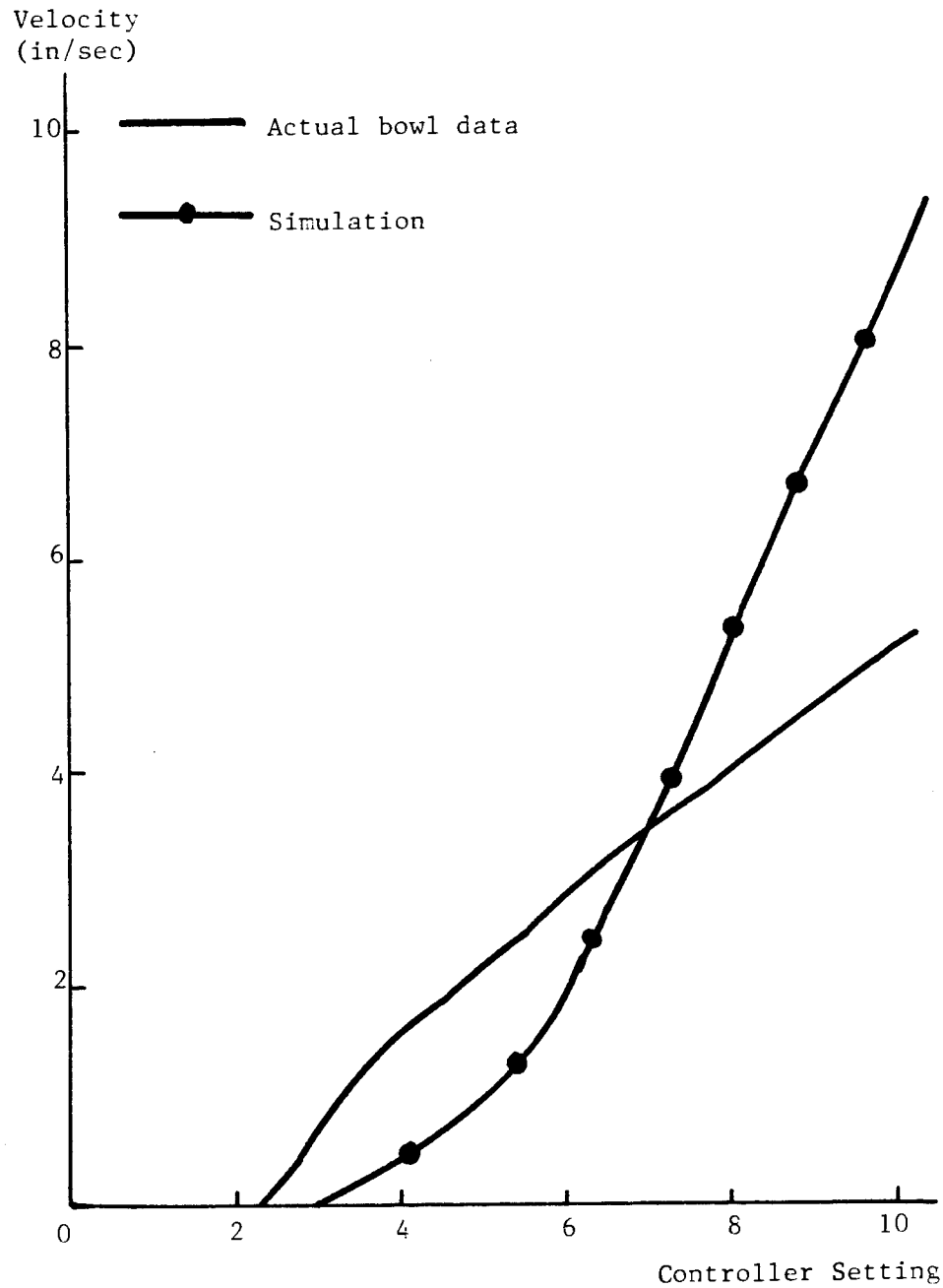

Figure 26: Velocity graph for ¼" hex nuts

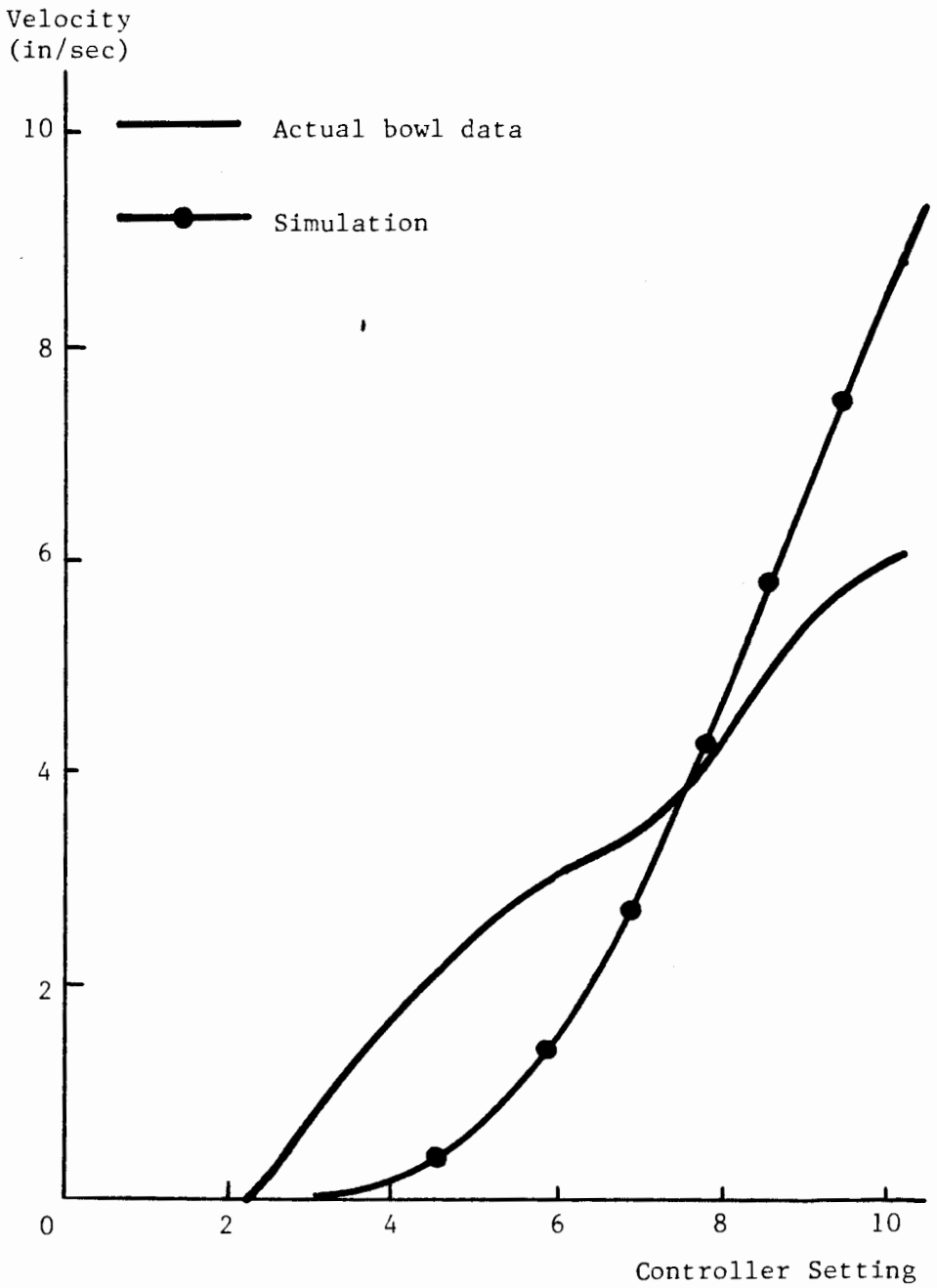

Figure 27: Velocity graph for 5/16" screws

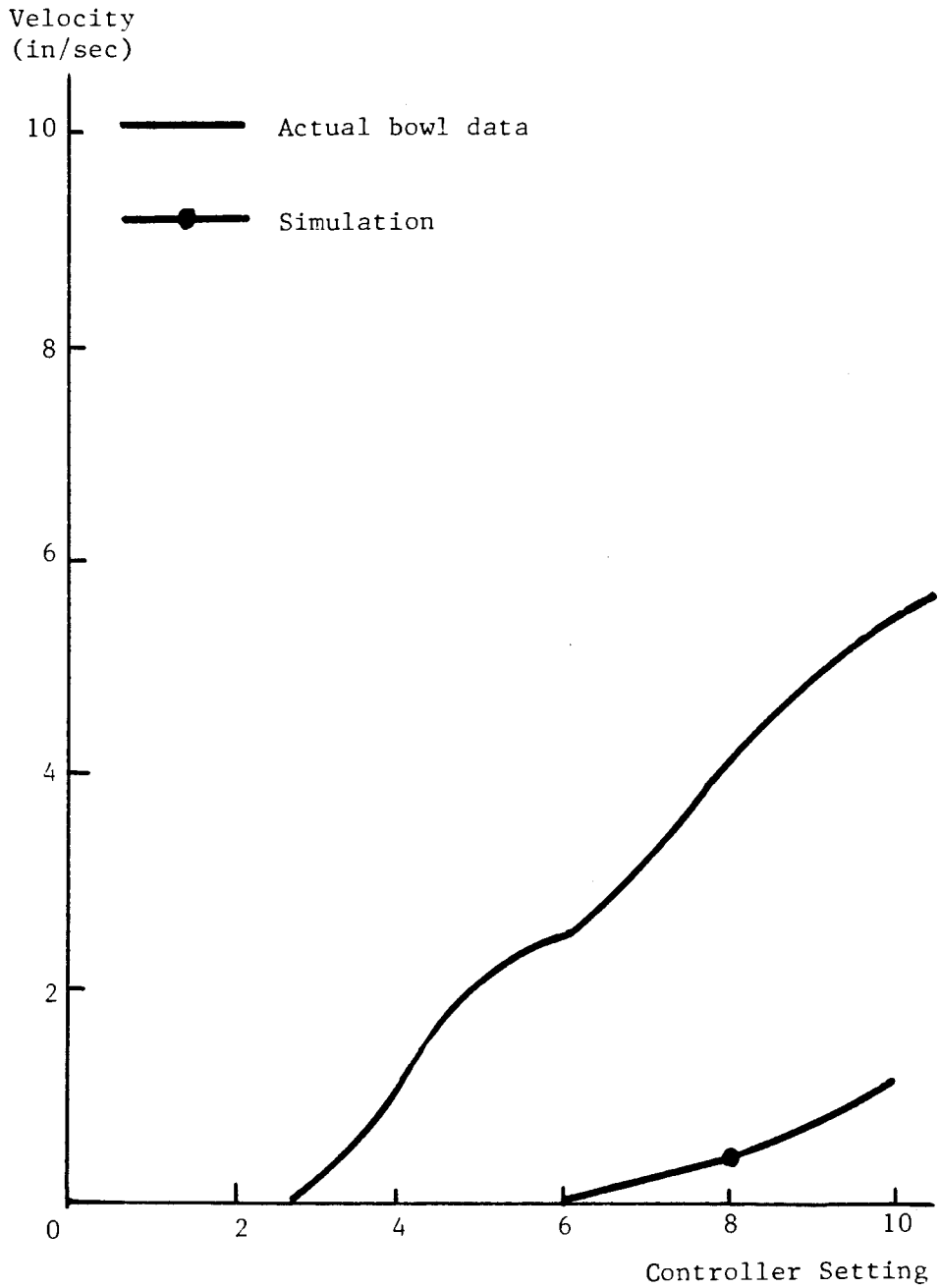

Figure 28: Velocity graph for 5/8" screws

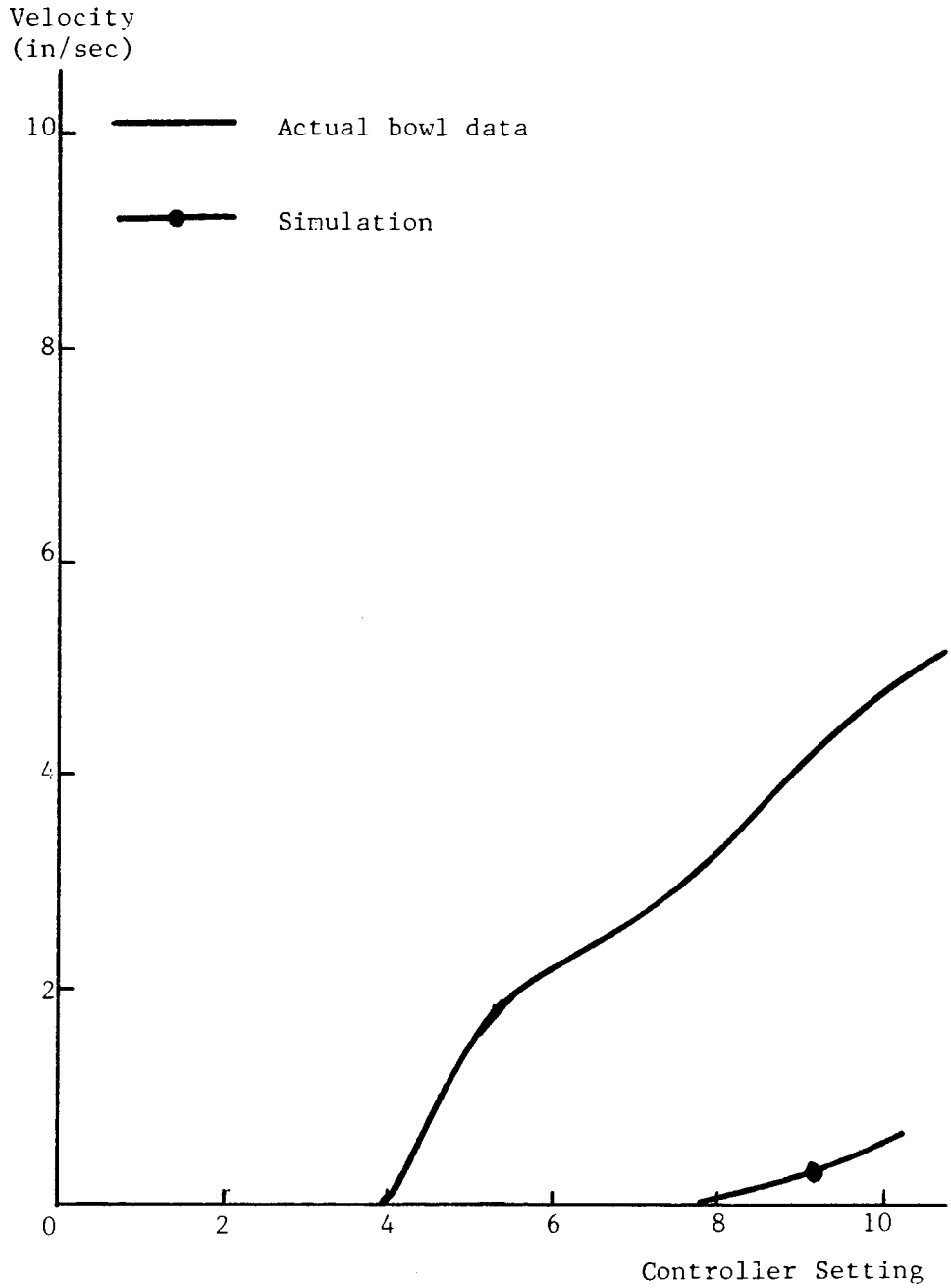

Figure 29: Velocity graph for 3/4" screws

Figure 30 shows velocity sensitivity to the weight of parts for 2 controller settings: 7 and 10. This graph confirms the sensitivity of the simulation model to the weight of parts. It also shows the trend of velocities to increase for higher controller settings in both the actual and simulated runs. In this respect, the model does correlate with actual data.

For all bowl runs thus far, the number of parts has been equal to 25 on all runs. The weight in the bowl was not the same for every part. To test the effect of part differences on feed rates, an equal weight of parts was placed in the bowl for 3 part types. A weight of .3 pounds of parts was placed in the bowl for crimp terminals, 5/16-inch screws, and 3/4-inch screws, and velocities measured at various controller settings. Figure 31 is a graph of actual and simulated velocities at a controller setting of 7. The simulation predicts equal velocities for equal bowl masses independent of individual part size. Actual bowl data closely approximates simulated data, indicating that total bowl weight probably effects feed rate more than individual part weight.

The graphs in figures 24 through 31 indicate that, although the simulation model can predict general trends in the data, it cannot predict precise part velocities. Possible reasons for this weakness in the model can be found in some of the assumptions made during it's derivation.

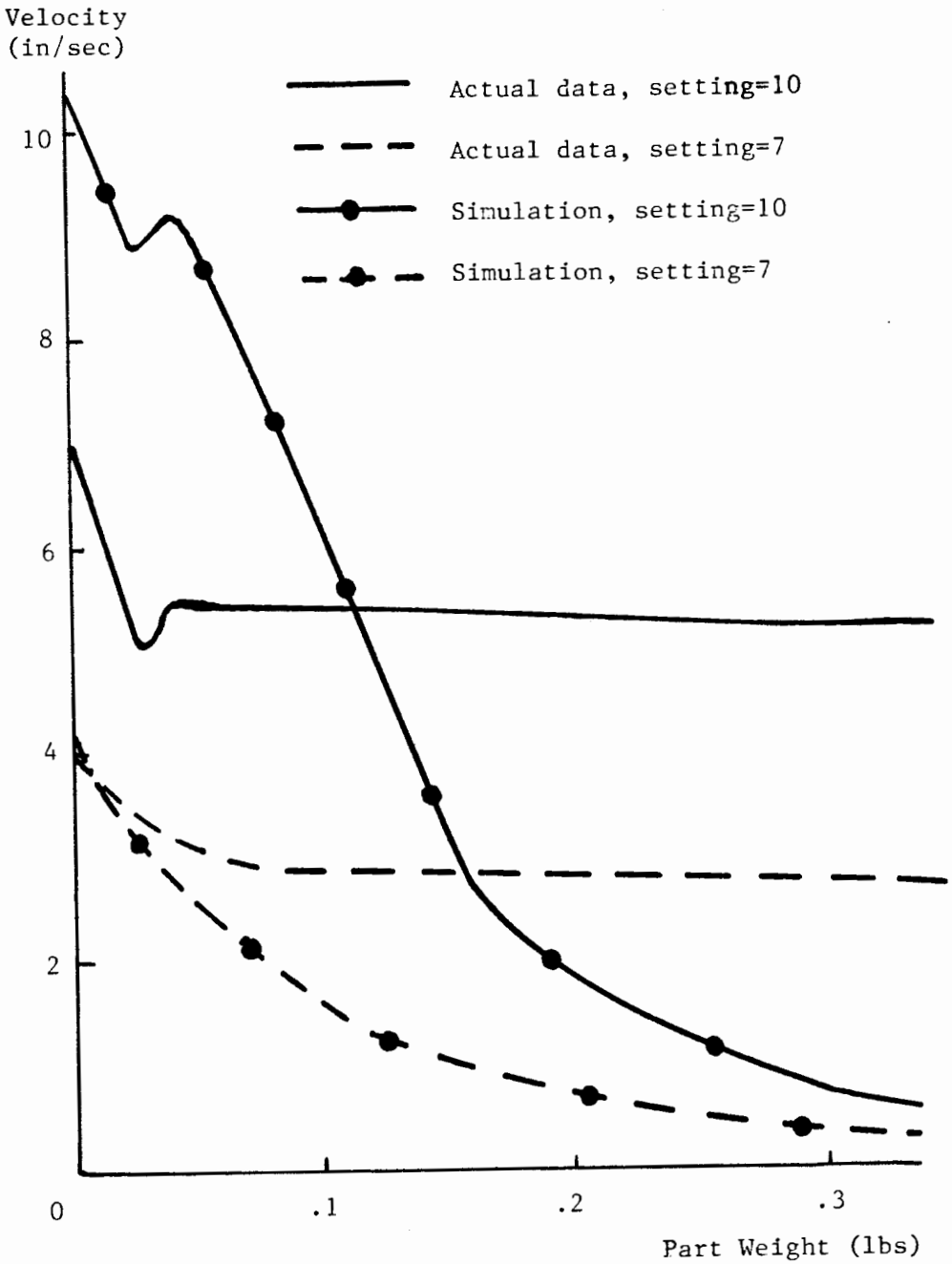

Figure 30: Part velocity versus part weight

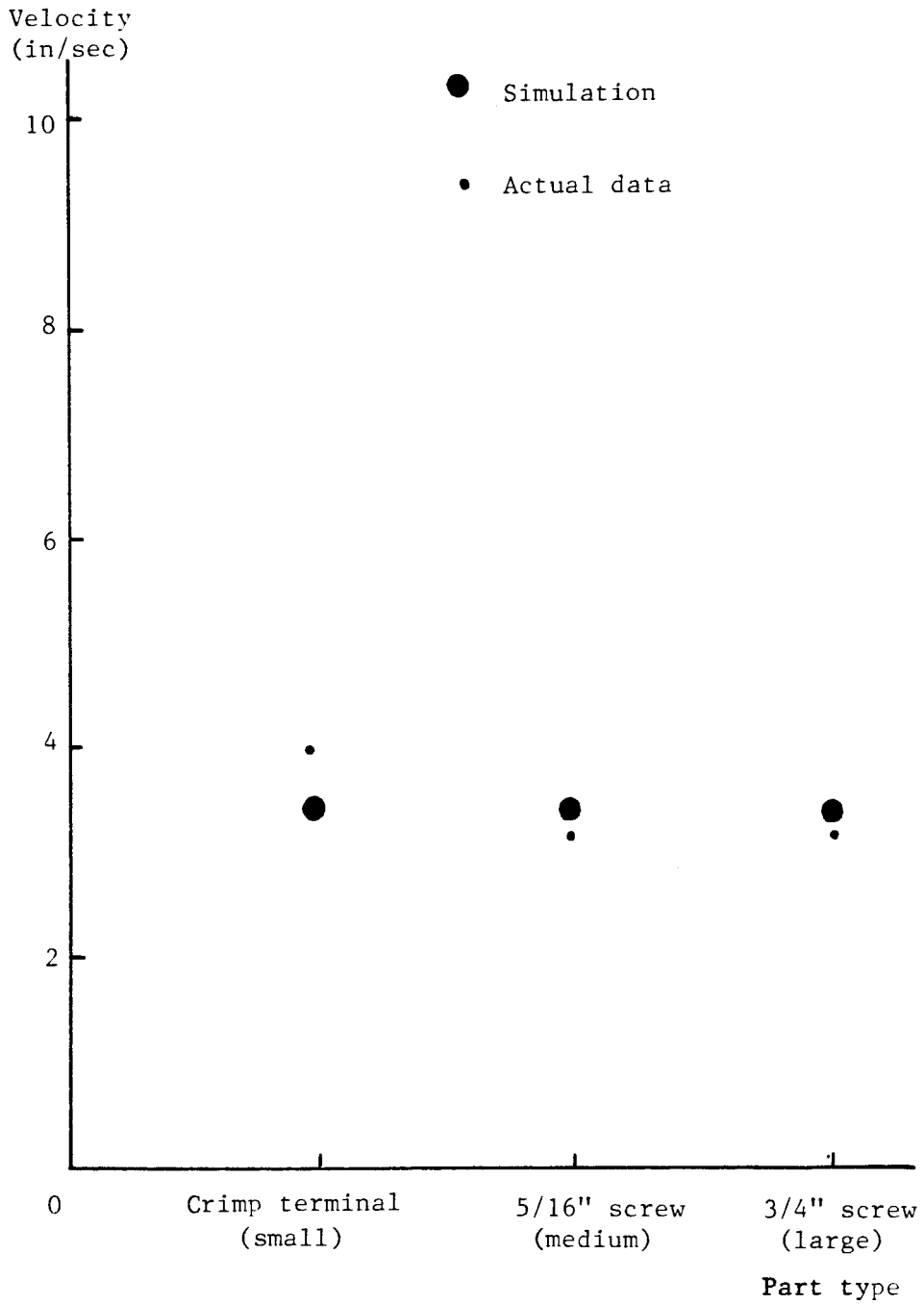

Figure 31: Part velocity sensitivity to part type

A major assumption made during the model's derivation involved linearity of the track. The movement of the part was simplified to motion in a straight line, when in reality the part moves radially along the helical bowl track. The actual path of the part is circular, due to its contact with the bowl sidewall. The frictional forces acting between the part and the sidewall were not included in the model, which may account for some of the error between the simulation results and the actual data.

Another important assumption involved the hopping behavior of the part. After the part hit the bowl surface, an inelastic collision was assumed between the part and the track. This assumption may be too strict, since physical parts may bounce on the bowl track following impact. These elastic collisions could greatly effect actual part feed rates, which may be another source of error in the simulation results.

When deriving the systems dynamics equations for bowl motion, the bowl was treated as a solid mass. The force exerted by the parts was treated as a constant. Physically, the parts exert a variable force on the bowl due to the fact that they are not attached to the bowl. This phenomenon was not included in the bowl model, but was simplified and treated as a constant force.

The discrepancies between the simulation and real world results may also be due to physical aspects of the bowl not

accounted for in the model. One of these properties is the gap clearance between the electromagnet and the steel plate on the bottom of the bowl. The sensitivity of electromagnetic forces to this gap clearance is unknown. As mentioned in chapter 4, during the measurement of this force, the gap setting was at .020 inches. During the gathering of part velocity data, the gap setting was around 0.18 inches. This difference in gap clearance may have had some impact on the resultant electromagnetic force, creating some difference between simulated and actual drive inputs.

Finally, the bowl was found to be very sensitive to the screws mounting the bowl to the springs. Tightening these screws greatly increased feed rates. This factor made part velocities more difficult to predict due to uncertainty regarding the optimal tightness of the screws.

Chapter VI

CONCLUSIONS

The objective of this research was to develop a model of the bowl feeder and use it to gain knowledge about multi-variable feeding relationships. A systems model was developed using dynamics to model the bowl's vibration as well as the part's movement. This model was input into a simulation program and compared to actual part velocities in a physical feeder. The results showed that the model could predict trends in the data, but not exact part velocities.

Some general conclusions were made about the mass of the parts in the bowl. Light weights of parts in the bowl feed faster than heavy weights, indicating that as the bowl empties, the feed rate of parts will increase. Also, the total weight of the parts in the bowl effects feed rate more greatly than the individual weights of the parts.

During the verification in chapter 5 only the mass of parts was changed to test the model. Theoretically, any parameter could be changed in the model and tested. Several parameters were varied in the model only and the results recorded.

The first parameter studied the frequency of current input to the system. The simulation's output is graphed in figure 32. This data was calculated with the same parameters used throughout the research (from Table 4), including a controller setting of 10, the mass of a part equal to .025 pounds, and the number of parts being 10. The graph shows that there is an optimal frequency range. A frequency of 45 hertz appears to be optimal for this set of parameters. The shape of this curve makes sense, since at very low frequencies, conveying velocities are low, and at high frequencies, excessive bouncing of parts hampers feed rate. These results contradict the research of Boothroyd and Redford (7), who claim that feed rate is inversely proportional to conveying velocity. However, DeCock suggests that frequency does behave as shown in figure 32 (9).

Other parameters tested include the vibration angle, Ψ, as well as the static and kinetic coefficients of friction, μ_s and μ_k, respectively. Using standard parameters again, the velocity results are graphed in figure 33. This shows that an optimal vibration angle exists for several frictional coefficients, it's magnitude being around 20 degrees. Research at Ohio State by Hildebrand on a horizontal belt feeder showed that the optimal belt angle was 18 degrees (15), which is a measure similar to Ψ. In addition, the graph shows that higher coefficients of friction generate higher part velocities over the majority

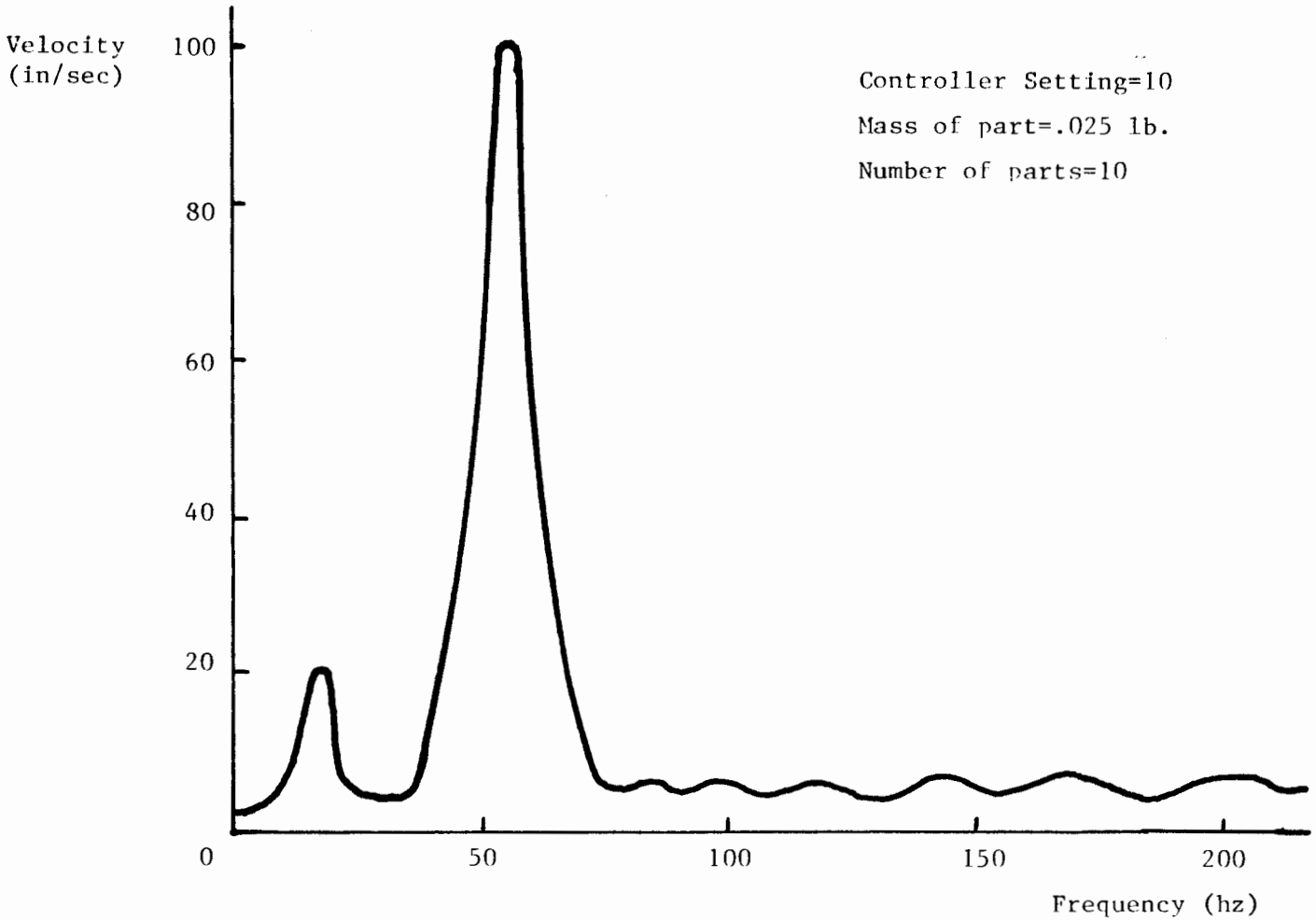

Figure 32: Velocity as a function of frequency

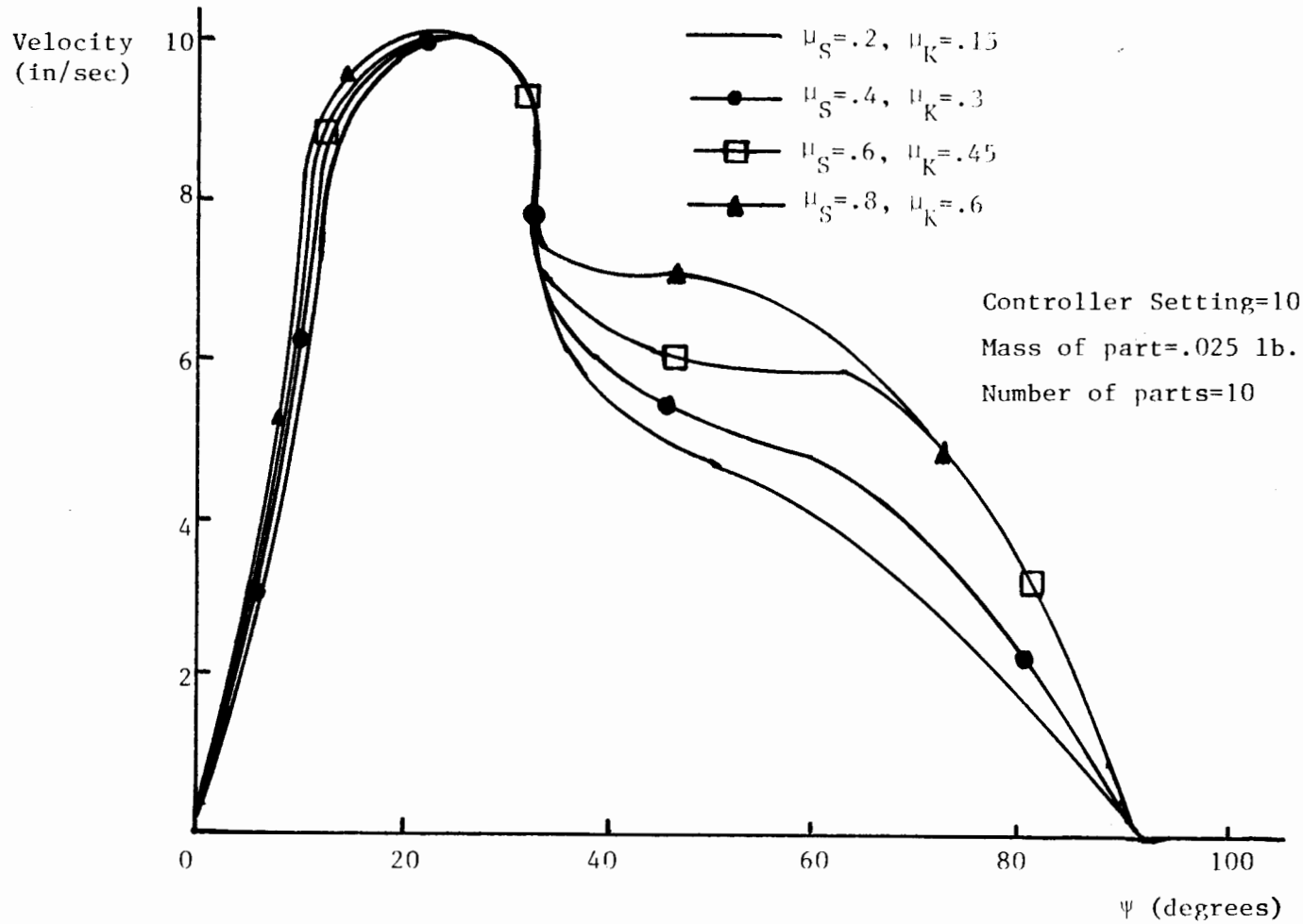

Figure 33: Effect of vibration angle on velocity for several frictional coefficients

of Ψ values. These results concur with those of Boothroyd and Redford regarding the effect of vibration angle on conveying velocities for various frictional coefficients (7).

These theoretical results indicate that the simulation model can predict the effects of changes in various parameters. Although actual part velocities are incorrect, the trends of the simulated data agree with previous research and expected physical effects. In this respect, the model is useful in determining the effects of multi-variable feeding relationships.

Chapter VII

FUTURE RESEARCH

Suggested future research in the area of modeling the motion of parts in a vibratory bowl feeder involves the assumptions presented in chapter 5. These assumptions should be dropped, and more explicit part behavior patterns developed. The effect of friction between the part and sidewall of the bowl should be modeled. An algorithm for elastic part/track collisions should be developed, as well as interactive forces for the parts in the bowl.

To insure uniformity in data, several bowl feeders should be used to gather data to test the variations of manufacturing and assembly that can effect a design's performance. By using several feeders the uncertainty regarding the effect of this variation can be eliminated by comparing it with averaged data.

The sensitivity of other parameters in the model should be tested and verified. Important parameters include k_1, the spring constant, b_1, the spring damping, as well as those parameters tested in this research but not verified: f, the frequency; ψ, the vibration angle, and μ_s and μ_k, the static and kinetic coefficients of friction.

The ultimate objective of this feeder simulation model is to determine optimal parameters in order to improve the design of bowl feeders. The model should be optimized so that results can be used to build an optimal vibratory bowl feeder.

BIBLIOGRAPHY

1. Akhmechet, L. S., O. I. Blakh, A. G. Matsieyenski, Ye. N. Nesterov, and S. Kh. Sviredenko, "Choice of Parameters for Vibratory Hoppers," Machines and Tooling, Vol. 30, No. 2, pp. 9-11 (1959).

2. Anonymous, "Feeders Solve a Lot of Problems," Production Engineering, Vol. 28, No. 3, pp. 66-71 (March 1981).

3. Anonymous, "Part Feeding is the Achilles Heel of Robot Assembly," Assembly Automation, Vol. 3, No. 3, pp. 74-77 (May 1983).

4. Anonymous, "Parts Handling Technology-Simple Solutions," Assembly Engineering, Vol. 26, No. 5, pp. 66-67 (May 1983).

5. Baumeister, Theodore, Eugene A. Avallone and Theodore Braumeister III, Mark's Standard Handbook for Mechanical Engineers, New York: McGraw-Hill Book Company (1978).

6. Boothroyd, Geoffrey, Corrado Poli, and Laurence Murch, Automatic Assembly, New York: Marcel Dekker Inc. (1982).

7. Boothroyd, G., and A. H. Redford, Mechanized Assembly, London: McGraw-Hill (1968).

8. Box, George E. P., William G. Hunter, and J. Stuart Hunter, Statistics for Experimenters, New York: John Wiley & Sons (1978).

9. DeCock, J. G., "Vibratory Feeders," Philips Technical Review, Vol. 24, No. 3, pp. 84-95 (1962/63).

10. Freier, George D., University Physics: Experiment and Theory, New York: Appleton-Century-Crafts (1965).

11. Gladfelter, Robert F., "Feeding and Orienting Parts," Automation, Vol. 15, No. 4, pp. 110-114 (April 1968).

12. Goodrich, Jerry L. and Gary Maul, "Programmable Parts Feeders," Industrial Engineering, Vol. 15, No. 5, pp. 28-33 (May 1983).

13. Haupt, B. J., "The Systems Approach to Automation in the Modern Plant," Proceedings from the 15th CIRP Seminar, (June 1983).

14. Heginbotham, W. B., D. F. Barnes, D. R. Purdue, and D. J. Law, "Flexible Assembly Module with Vision Controlled Placement Device," Proceedings of the 11th International Symposium on Industrial Robots, pp. 479-488 (October 1981).

15. Hildebrand, Joseph, Research and Development for Low Cost Programmable Feeding of Headed Parts Using Bi-Directional Belts, Unpublished Masters Thesis in Industrial and Systems Engineering, Ohio State University (1984).

16. Maul, Gary P., and Jerry L. Goodrich, "A Methodology for Developing Programmable Part Feeders," IIE Transactions, Vol. 15, No. 4, pp. 330-335 (December 1983).

17. Redford, A. H., and G. Boothroyd, "Vibratory Feeding," Proceedings of the Institute of Mechanical Engineers, Vol. 182, No. 6, pp. 135-152 (1967-1968).

18. Reswick, James B. and Charles K. Taft, Introduction to Dynamic Systems, Englewood Cliffs, New Jersey: Prentice-Hall (1967).

19. Ridings, James L., "The Challenges of the Factory of the Future," SME Technical Paper, No. MS82-395 (December 1982).

20. Riley, Frank J., "Product Design for Automatic Assembly," Proceedings from the 15th CIRP Seminar, (June 1983).

21. Smith, Floyd E., "Applying Vibratory Bowl-Type Feeders -Part 1," Automation, Vol. 9, No. 11, pp. 97-102 (November 1962).

22. Smith, Floyd E., "Applying Vibratory Bowl-Type Feeders - Part 2," Automation, Vol. 9, No. 12, pp. 79-85 (December 1962).

23. Tipping, W. V., An Introduction to Mechanical Assembly, London: Business Books Ltd. (1969).

24. Treer, Kenneth R., Automated Assemly, Dearborn, Michigan: Society of Manufacturing Engineers (1979).

Appendix

```
C*************************************************************************
C
C       THIS PROGRAM COMPUTES THE FEED RATES OF PARTS IN A VIBRATORY
C       BOWL FEEDER USING EULER'S APPROXIMATION.
C
C       VARIABLES
C       (MAIN PROGRAM)
C       U1OLD           PREVIOUS BOWL DISPLACEMENT, Z1
C       U2OLD           PREVIOUS BOWL VELOCITY
C       U3OLD           PREVIOUS BASE DISPLACEMENT, Z2
C       U4OLD           PREVIOUS BASE VELOCITY
C       U1NEW           CURRENT BOWL DISPLACEMENT, Z1
C       U2NEW           CURRENT BOWL VELOCITY
C       U3NEW           CURRENT BASE DISPLACEMENT, Z2
C       U4NEW           CURRENT BASE VELOCITY
C       W1OLD           PREVIOUS PART DISPLACEMENT, XP
C       W2OLD           PREVIOUS PART VELOCITY
C       W1NEW           CURRENT PART DISPLACEMENT, XP
C       W2NEW           CURRENT PART VELOCITY
C       Y1OLD           PREVIOUS PART NORMAL DISPLACEMENT
C       Y2OLD           PREVIOUS PART NORMAL VELOCITY
C       Y1NEW           CURRENT PART NORMAL DISPLACEMENT
C       Y2NEW           CURRENT PART NORMAL VELOCITY
C       Z1AOLD          PREVIOUS BOWL ACCELERATION
C       Z1ANEW          CURRENT BOWL ACCELERATION
C       XPANEW          CURRENT PART ACCELERATION
C       FNOLD           PREVIOUS NORMAL FORCE
C       FNNEW           CURRENT NORMAL FORCE
C       VLTFRC          VOLTAGE FORCE APPLIED
C       FRCFNC          OUTPUT OF VOLTAGE STEP FUNCTION
C       FINERT          INERTIAL FORCE
C       LIMIT           DURATION OF SIMULATION
C       N               NUMBER OF CYCLES
C       MUSTAT          COEFFICIENT OF STATIC FRICTION
C       MUKIN           COEFFICIENT OF KINETIC FRICTION
C       MASS1           MASS OF BOWL AND PARTS
C       MASS2           MASS OF BASE
C       MASSP           MASS OF PART
C       PARTNM          NUMBER OF PARTS IN BOWL
C       K1              SPRING CONSTANT, BOWL TO BASE
C       K2              SPRING CONSTANT, BASE TO GROUND
C       B1              DAMPING, BOWL TO BASE
C       B2              DAMPING, BASE TO GROUND
C       VOLT            VOLTAGE SETTING APPLIED
C       FREQ            FREQUENCY OF VOLTAGE INPUT
C       PSI             ANGLE OF VIBRATION
C       THETA           ANGLE OF INCLINATION
C       DELTA           TIME DIFFERENTIAL
C       G               GRAVITY
C       T               TIME
C       ISTAGE          PART MOTION STAGE
C       NEXT            STAGE NUMBER ON NEXT CYCLE
C       Aij             COEFFICIENTS OF BOWL EQUATION MATRIX
C
C       (SUBROUTINE STEP)
C       ONOFF           DETERMINES IF OUTPUT 0 OR VOLTAGE FORCE
C       FLIP            CHANGES SIGN AFTER EACH DIFFERENT OUTPUT
C       INDEX           TIME INDEX
C       OLDSTP          PREVIOUS OUTPUT
C
C       INPUT INFORMATION
C
```

```
C       ALL ANGLES ARE INPUT IN DEGREES, AND CONVERTED IN PROGRAM
C       ALL INPUT VALUES ARE REAL
C
C       FILES CREATED: VELOC.DAT
C
C*******************************************************************************
C
        REAL LIMIT,MUSTAT,MUKIN,MASSP,MASS1,MASS2,K1,K2,B1,B2,PSI,INDEX
C
C       **      INPUT PARAMETERS
C
        OPEN(UNIT=1,FILE='VELOC.DAT',STATUS='UNKNOWN')
        TYPE 801
  801   FORMAT(' ','INPUT: MUSTAT,MUKIN,M1,K1,B1')
        READ(5,901) MUSTAT,MUKIN,MASS1,K1,B1
  901   FORMAT(2(F5.3),F9.5,2(F9.3))
        TYPE 802
  802   FORMAT(' ','INPUT: FREQ,VOLT SETTING,MASSP,NUM. PARTS')
        READ(5,990) FREQ,VOLT,MASSP,PARTNM
  990   FORMAT(F5.1,F6.2,F10.8,F6.0)
        TYPE 803
  803   FORMAT(' ','INPUT: PSI,THETA,M2,K2,B2')
        READ(5,991) PSI,THETA,MASS2,K2,B2
  991   FORMAT(F5.2,F5.2,F9.5,2(F9.3))
        TYPE 804
  804   FORMAT(' ','INPUT: DELTA,LIMIT')
        READ(5,992) DELTA,LIMIT
  992   FORMAT(F7.6,F4.2)
        WRITE(1,902) MUSTAT,MASS1,K1,B1,FREQ
        WRITE(1,903) VOLT,PARTNM,PSI,THETA,MASS2
        WRITE(1,904) K2,B2,DELTA,LIMIT
        WRITE(1,929) MUKIN,MASSP
C       WRITE(1,905)
        WRITE(1,906)
  902   FORMAT(' ',T5,'MUSTAT=',F5.3,T18,'M1=',F9.5,T31,'K1=',F9.3,T44,
     $            'B1=',F9.3,T57,'FREQ=',F5.1)
  903   FORMAT(' ',T5,'VSET=',F6.2,T18,'NMPRT=',F6.0,T31,'PSI=',F5.2,T44,
     $            'TH=',F5.2,T57,'M2=',F9.5)
  904   FORMAT(' ',T5,'K2=',F9.3,T18,'B2=',F9.3,T31,'DEL=',F7.6,T44,
     $            'LIM=',F4.2)
  929   FORMAT(' ',T5,'MUKIN=',F5.3,T18,'MASSP=',F10.8)
  906   FORMAT(' ')
C
C       **      INITIALIZE VARIABLES
C
        U1OLD=0.
        U2OLD=0.
        U3OLD=0.
        U4OLD=0.
        Z1AOLD=0.
        FNOLD=0.
        W1OLD=0.
        W2OLD=0.
        G=32.174*12.
        MASS1=MASS1/G
        MASS2=MASS2/G
        MASSP=MASSP/G
        MASS1=MASS1+(MASSP*PARTNM)
        T=0.
        ONOFF=1.
        FLIP=1.
        INDEX=0.
```

```
      OLDSTP=0.
      N=INT(LIMIT/DELTA)
      PI=3.141592654
      PSI=PSI*PI/180.
      THETA=THETA*PI/180.
      A11=0.
      A12=1.
      A13=0.
      A14=0.
      A21=-(K1/MASS1)
      A22=-(B1/MASS1)
      A23=(K1/MASS1)
      A24=(B1/MASS1)
      A31=0.
      A32=0.
      A33=0.
      A34=1.
      A41=(K1/MASS2)
      A42=(B1/MASS2)
      A43=(-K1-K2)/MASS2
      A44=(-B1-B2)/MASS2
      NEXT=3
      VLTFRC=(.901*(VOLT**2))-(.896*VOLT)+1.724
      FRCFNC=VLTFRC
      JK=0
C
C     **      LOOP THROUGH EQUATIONS
C
      DO 10 I=1,N
C
C     **      BOWL MOTION
C
            U1NEW=U1OLD+(DELTA*U2OLD)
            U2NEW=((A21*DELTA)*U1OLD)+
     $            (((A22*DELTA)+1.)*U2OLD)+
     $            ((A23*DELTA)*U3OLD)+
     $            ((A24*DELTA)*U4OLD)+
     $            ((FRCFNC*DELTA)/MASS1)
            U3NEW=U3OLD+(DELTA*U4OLD)
            U4NEW=((A41*DELTA)*U1OLD)+
     $            ((A42*DELTA)*U2OLD)+
     $            ((A43*DELTA)*U3OLD)+
     $            (((A44*DELTA)+1.)*U4OLD)
            T=T+DELTA
            FRCFNC=STEP(T,ONOFF,FLIP,INDEX,OLDSTP,VLTFRC,FREQ)
            Z1ANEW=(A21*U1NEW)+(A22*U2NEW)+(A23*U3NEW)+
     $             (A24*U4NEW)+(FRCFNC/MASS1)
            FNNEW=(MASSP*G*COS(THETA))+(MASSP*(-Z1ANEW)*SIN(PSI))
            IF (FNNEW.LT.0.) FNNEW=0.
            GO TO (11,22,33,44), NEXT
C
C     **      PART MOTION: FORWARD
C
   11       W2NEW=W2OLD+DELTA*(-(G*SIN(THETA))-((MUKIN/
     $            MASSP)*FNOLD))
            IF (FNNEW.LE.0.) THEN
                  NEXT=4
                  Y2NEW=(-U2NEW)*SIN(PSI)
                  Y1NEW=(-U1NEW)*SIN(PSI)
            ELSE  IF ((-U2NEW)*COS(PSI).GE.W2NEW) THEN
                        NEXT=3
                  ELSE
```

```
                                        NEXT=1
                        END IF
                        ISTAGE=1
                        GO TO 55
C
C       **      PART MOTION: BACKWARD
C
   22           CONTINUE
                        W2NEW=W2OLD+DELTA*(-(G*SIN(THETA))+((MUKIN/
     $                        MASSP)*FNOLD))
                        IF (FNNEW.LE.0.) THEN
                                NEXT=4
                                Y2NEW=(-U2NEW)*SIN(PSI)
                                Y1NEW=(-U1NEW)*SIN(PSI)
                        ELSE    IF ((-U2NEW)*COS(PSI).LE.W2NEW) THEN
                                        NEXT=3
                                ELSE
                                        NEXT=2
                        END IF
                        ISTAGE=2
                        GO TO 55
C
C       **      PART MOTION: STATIONARY
C
   33           CONTINUE
                        W2NEW=(-U2NEW)*COS(PSI)
                        XPANEW=(-Z1ANEW)*COS(PSI)
                        FINERT=(MASSP*XPANEW)+(MASSP*G*SIN(THETA))
                        IF (FNNEW.LE.0.) THEN
                                NEXT=4
                                Y2NEW=(-U2NEW)*SIN(PSI)
                                Y1NEW=(-U1NEW)*SIN(PSI)
                        ELSE    IF ((MUSTAT*FNNEW).GT.ABS(FINERT)) THEN
                                        NEXT=3
                                ELSE    IF ((-U2NEW).GT.0.) THEN
                                                NEXT=2
                                        ELSE
                                                NEXT=1
                        END IF
                        ISTAGE=3
                        GO TO 55
C
C       **      PART MOTION: HOP
C
   44           CONTINUE
                        W2NEW=W2OLD+DELTA*(-(G*SIN(THETA)))
                        Y1NEW=Y1OLD+(DELTA*Y2OLD)
                        Y2NEW=Y2OLD+(DELTA*(-G*COS(THETA)))
                        IF ((-(U1NEW*SIN(PSI))).LT.Y1NEW) THEN
                                NEXT=4
                        ELSE
                                NEXT=1
                        END IF
                        ISTAGE=4
   55           CONTINUE
                W1NEW=W1OLD+(DELTA*W2OLD)
C
C       **      WRITE TO FILE; UPDATE VARIABLES
C
                IF (MOD(JK,500).EQ.0) THEN
                        WRITE(1,558) ISTAGE,(-Z1ANEW)
  558                   FORMAT('0',T2,'STAGE=',I2,T20,'A1=',F13.7)
```

```
                        WRITE(1,907) T,W1NEW,W2NEW,FRCFNC
  907                   FORMAT(' ',T2,'TIME=',F7.6,T20,'XP=',F13.7,T38,
     $                         'VP=',F13.7,T56,'VLTFRC=',F8.4)
                        WRITE(1,996) U1NEW,U2NEW,U3NEW,U4NEW
  996                   FORMAT(' ',T2,'X1=',F13.7,T20,'V1=',F13.7,T38,
     $                         'X2=',F13.7,T56,'V2=',F13.7)
                END IF
                U1OLD=U1NEW
                U2OLD=U2NEW
                U3OLD=U3NEW
                U4OLD=U4NEW
                Z1AOLD=(-Z1ANEW)
                FNOLD=FNNEW
                W1OLD=W1NEW
                W2OLD=W2NEW
                Y1OLD=Y1NEW
                Y2OLD=Y2NEW
                OLDSTP=FRCFNC
                JK=JK+1
   10   CONTINUE
        WRITE(5,810) W1NEW
  810   FORMAT(' ',F8.5)
        CLOSE(1)
        STOP
        END
C
C       **      FUNCTION STEP COMPUTES THE DRIVING STEP FORCE
C
        FUNCTION STEP(T,ONOFF,FLIP,INDEX,OLDSTP,VLTFRC,FREQ)
        REAL INDEX
        IF (T .GE. INDEX) THEN
                STEP=VLTFRC*ONOFF
                FLIP=-FLIP
                ONOFF=FLIP+ONOFF
                INDEX=INDEX+(1./(2.*FREQ))
        ELSE
                STEP=OLDSTP
        END IF
        END
```